Reconciling Deformation/Stressing Rate Models

Community Stress Workshop

May 29, 2013

Assumptions:

- strain rate can be converted to stress rate using some rheology
- surface stress rate can be downward continued to seismogenic depth

Comparison of 17 strain rate models

Selection of 5 similar models

Coherence analysis of 4 models to establish spatial resolution

Comparison of 4 models with Yang EQ orientations

Where do we go from here?

Comparison of Strain-Rate Maps of Western North America

Thorsten Becker, University of Southern California
Peter Bird, University of California at Los Angeles
Jayne Bormann and Bill Hammond, UNR
Andrew Freed, Purdue University
Matthias Hackl, LMU, Munich, Germany
Brendan Meade and Jack Loveless, Harvard
William Holt, State University of New York, Stony Brook
Ben Hooks, University of Texas at El Paso
Sharon Kedar, Sean Baxter, JPL
Corne Kreemer, University of Nevada
Rob McCaffrey, Rensselaer Polytechnic Institute
Tom Parsons, USGS
Fred Pollitz, USGS Menlo Park
Zeng-Kang Shen, UCLA
Bridget Smith-Konter, University of Texas at El Paso
Carl Tape, Harvard
Yuehua Zeng, USGS

Limitations of GPS data

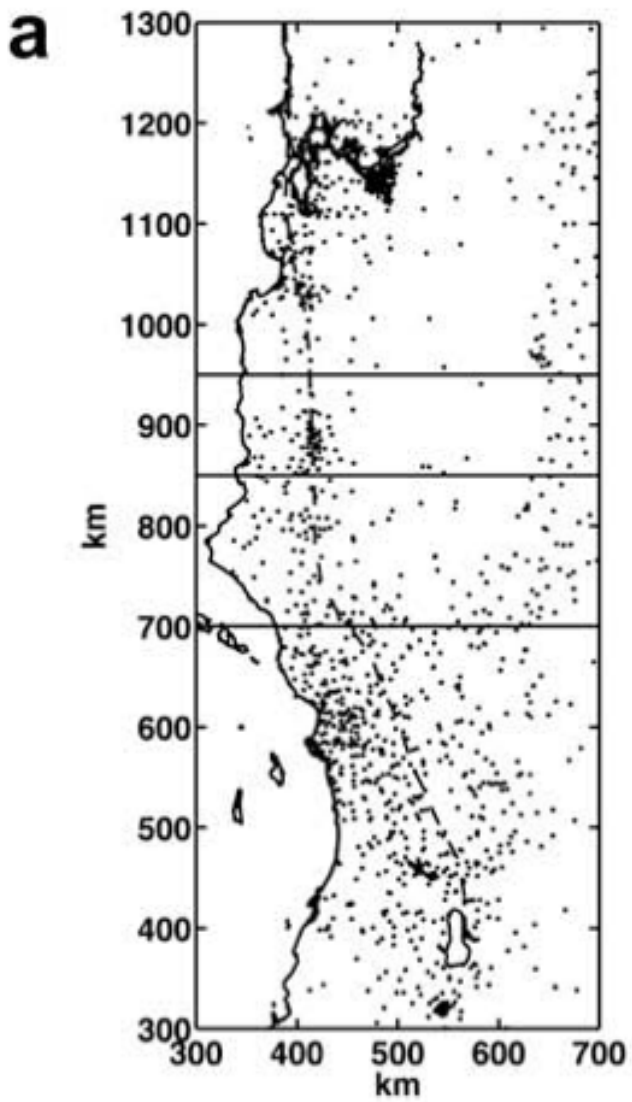

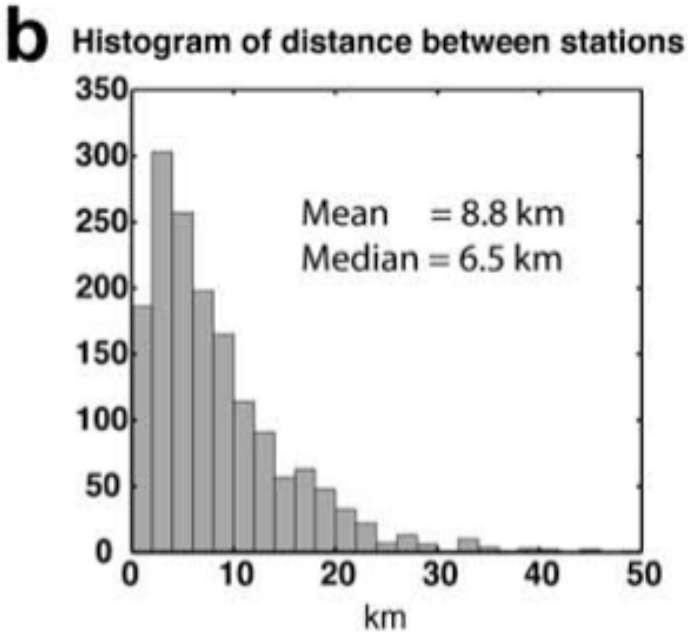

wavelengths < 13 km not resolved

wavelengths < 36 km poorly resolved

[Wei et al., 2010]

Velocity to Strain Rate

$v_i\left(x_j^k\right) \pm \sigma_i^k$ - vector velocity at point *k*

$i = 1,2,3 \quad j = 1,2 \quad k = 1 - N$

⇓ 2-D interpolation and/or dislocation model

$v_i\left(x_j\right)$ - surface vector velocity (0.01˚)

⇓ differentiation (GMT grdgradient)

$$\dot{\varepsilon}_{ij} = \frac{1}{2}\left(\frac{\partial v_i}{\partial x_j} + \frac{\partial v_j}{\partial x_i}\right)$$ - 2D strain rate

principal strain rate

$$\dot{\varepsilon}_{1,2} = \frac{\dot{\varepsilon}_{xx} + \dot{\varepsilon}_{yy}}{2} \pm \frac{1}{2}\left\{\left(\dot{\varepsilon}_{xx} - \dot{\varepsilon}_{yy}\right)^2 + 4\dot{\varepsilon}_{xy}^2\right\}^{1/2}$$

dilatation rate + maximum shear rate

second invariant

$$\dot{\varepsilon}_{II} = \left(\dot{\varepsilon}_{xx}^2 + \dot{\varepsilon}_{yy}^2 + 2\dot{\varepsilon}_{xy}^2\right)^{1/2}$$

Different Methods and Assumptions to Overcome Incomplete Spatial Sampling

Four approaches are used:

1) isotropic interpolation;
2) interpolation guided by known faults;
3) interpolation of a rheologically-layered lithosphere, and
4) model fitting using deep dislocations in an elastic layer or half space.

This living analysis compares strain rate maps from several groups to establish the common features among the maps, as well as the differences between the maps. These differences reveal the spatial resolution limitations of the GPS array, as well as assumed fault locations and rheological assumptions. Moreover the comparisons promote collaboration among the various groups to establish the best possible strain-rate map.

kedar_baxter

062 ηs

Strain rates calculated with a 30km Gaussian weighting radius per our scheme, generally following the formulation of Feigl et al [1993], i.e., there is no tectonic model involved, just a weighted least squares estimation at every point in the continuum.The attached images of the shear strain field were generated using progressively larger Guassian weighing radius plotted on the same amplitude color scale.

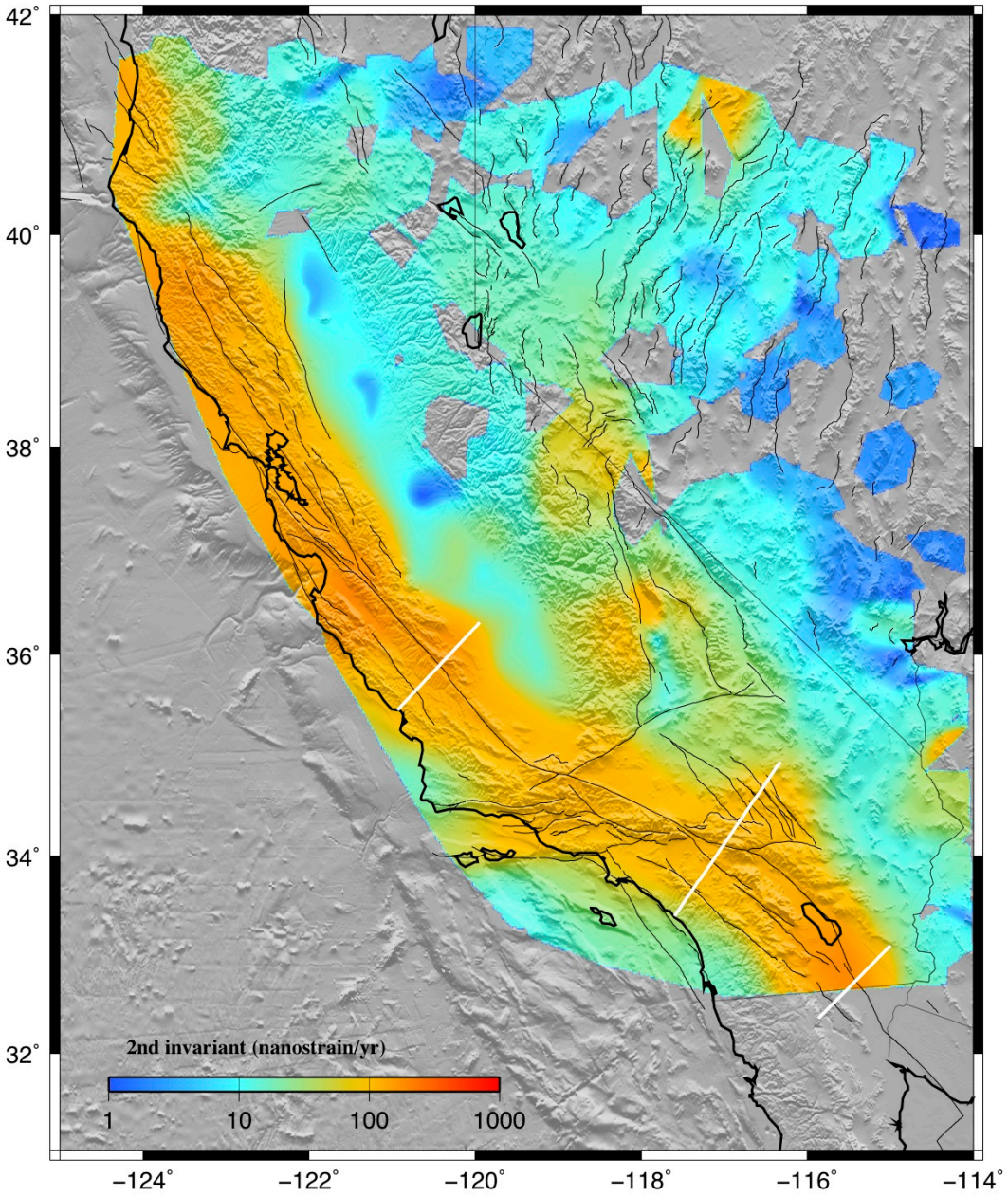

freed

064 ηs

Strain rates were derived based on 810 SCEC 3 velocity vectors (http://epicenter.usc.edu/cmm3/). We linearly interpolated the velocity data to an evenly spaced grid with increments of 0.1 degrees across the region using a weighted nearest neighboring scheme to dampen any locally sharp velocity contrasts. For grid points outside of the SCEC 3 region, we extrapolated the velocity field based on a fixed North America plate and a Pacific plate with a velocity of 48 mm/yr. We then triangulated the evenly spaced grid points using Delaunay triangulation (e.g., Shewchuk, 1996), and the strain tensor is determined for each triangle using minimum norm least squares. Reference: Freed et al., 2007.

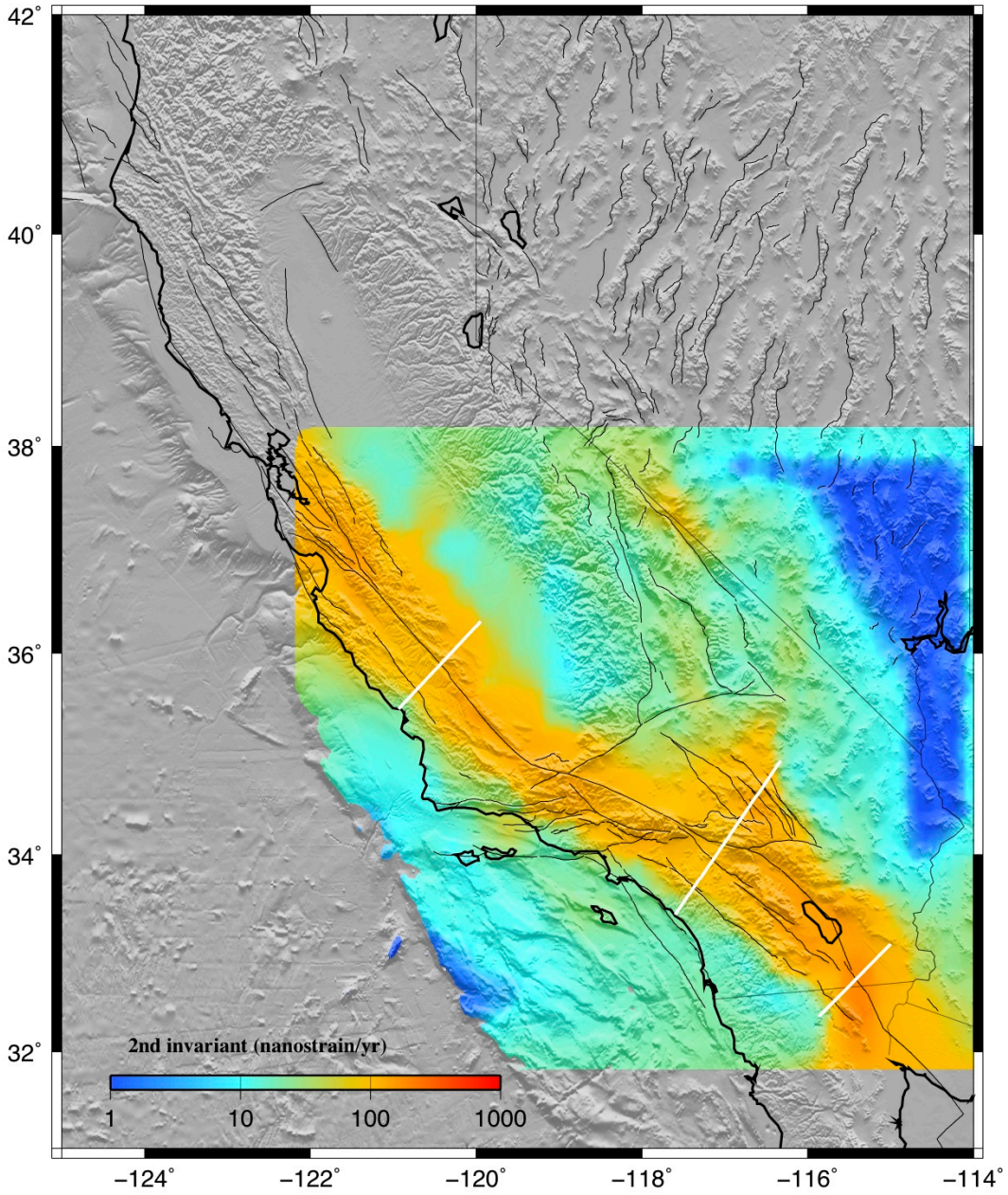

hooks

073 ηs

B.P. Hooks and B.R. Smith-Konter
Geological Sciences, Univ. of Texas – El Paso, El Paso, TX 79968

We present preliminary results of three-dimensional finite difference dynamic mechanical models. These models were completed using commercial software (Itasca, 2006; Fast Lagrangian Analysis of Continuum; FLAC^{3D}) that solves for large strains by utilizing simple stress – strain relationships and applied kinematic boundary conditions. The attached model results depart from a continuum through the inclusion of discontinuities that represent the major faults of the San Andreas Fault System. The model rheology is defined as a non-associated strain-weakening plasticity that allows for the localization of strain. A gridded PBO velocity is applied as a basal driving condition. The discontinuities behave according to the Coulomb sliding criteria and are assigned representative frictional properties. The solutions are produced through an explicit time-marching solution. The included data set (second invariant of the strain rate tensor; nanostrain/yr) is at 10 ky and at shallow depth (-2 km). Future iterations of this model will include dipping faults, topographically generated stress, pore fluid pressures, and temperature-dependent rheological models.

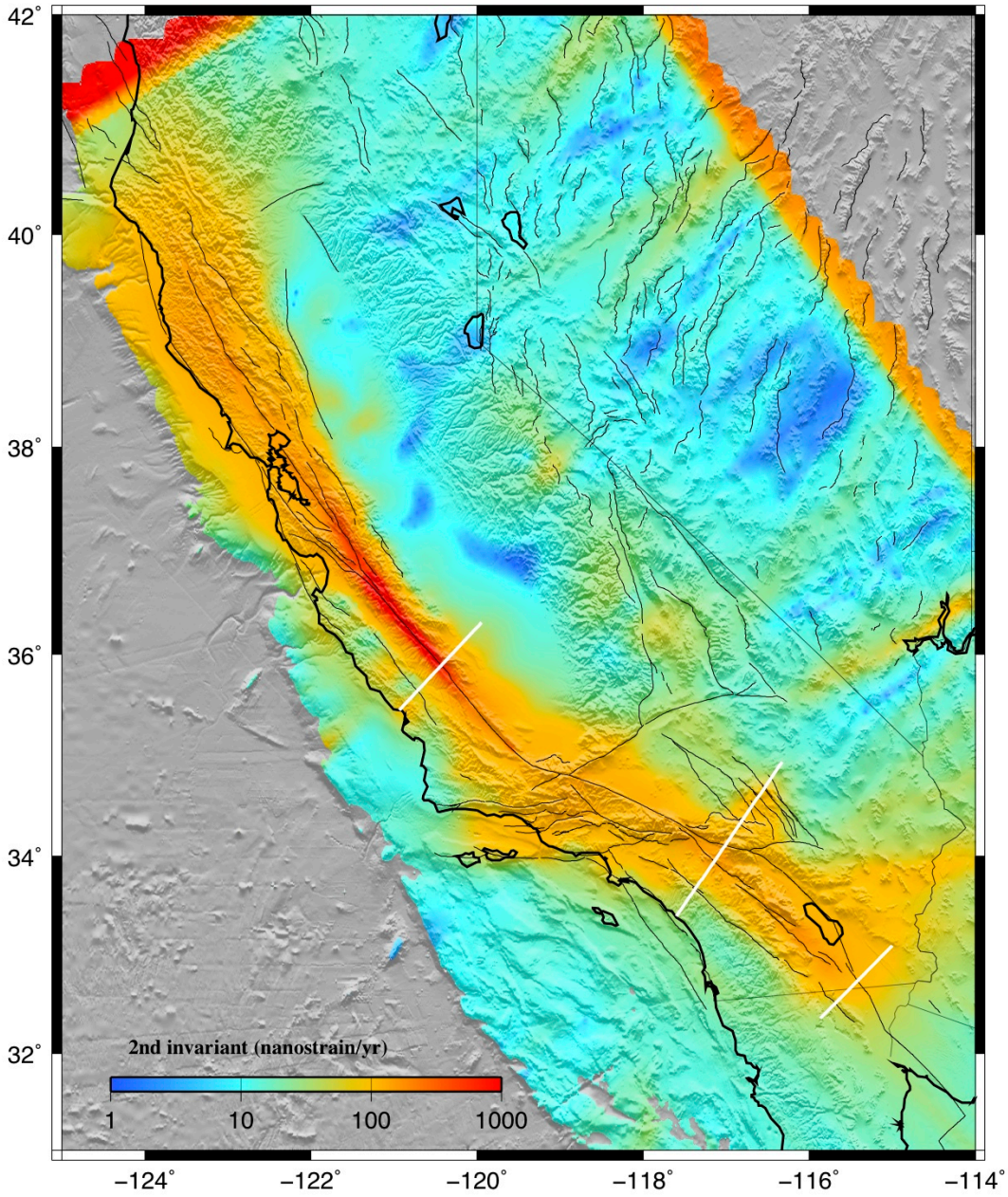

tape

074 ηs

Multiscale estimation of GPS velocity fields, C. Tape, P. Muse, M. Simons, D. Dong, and F. H. Webb, *Geophys. J. Int.*, 10.1111/j.1365-246X.2009.04337.x, 2009.

We present a spherical wavelet-based multiscale approach for estimating a spatial velocity field on the sphere from a set of irregularly spaced geodetic displacement observations. Because the adopted spherical wavelets are analytically differentiable, spatial gradient tensor quantities such as dilatation rate, strain rate and rotation rate can be directly computed using the same coefficients. In a series of synthetic and real examples,we illustrate the benefit of themultiscale approach, in particular, the inherent ability of the method to localize a given deformation field in space and scale as well as to detect outliers in the set of observations. This approach has the added benefit of being able to locally match the smallest resolved process to the local spatial density of observations, thereby both maximizing the amount of derived information while also allowing the comparison of derived quantities at the same scale but in different regions.We also consider the vertical component of the velocity field in our synthetic and real examples, showing that in some cases the spatial gradients of the vertical velocity field may constitute a significant part of the deformation. This formulation may be easily applied either regionally or globally and is ideally suited as the spatial parametrization used in any automatic time-dependent geodetic transient detector.

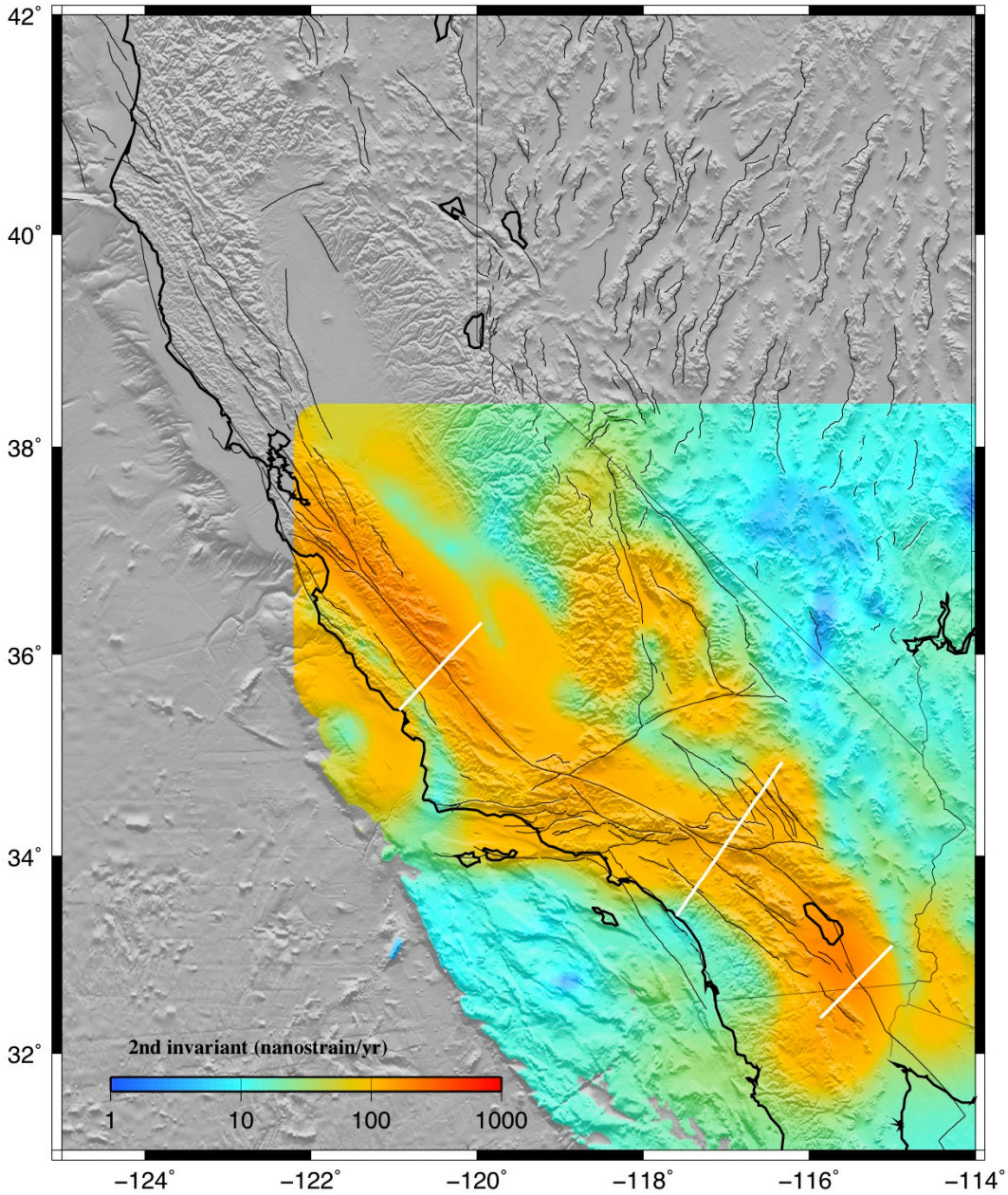

pollitz

080 ηs

Strain rates are derived by applying the isotropic interpolation method of Shen et al. (1996) to a compilation of 3650 horizontal GPS vectors in the western US. Contributing sources include PBO (714 vectors), Payne et al. (2008) (672 vectors), and various continuous and campaign GPS measurements (2264 vectors) such as USGS campaign data and the SCEC Crustal Motion Model 3.0. The Gaussian scaling distance used to weight velocity information in the Shen et al. method is here implemented as a function of position depending on the density of GPS measurements around a target point. This varies from 12 km in densely covered areas to 50 km in sparsely covered areas.

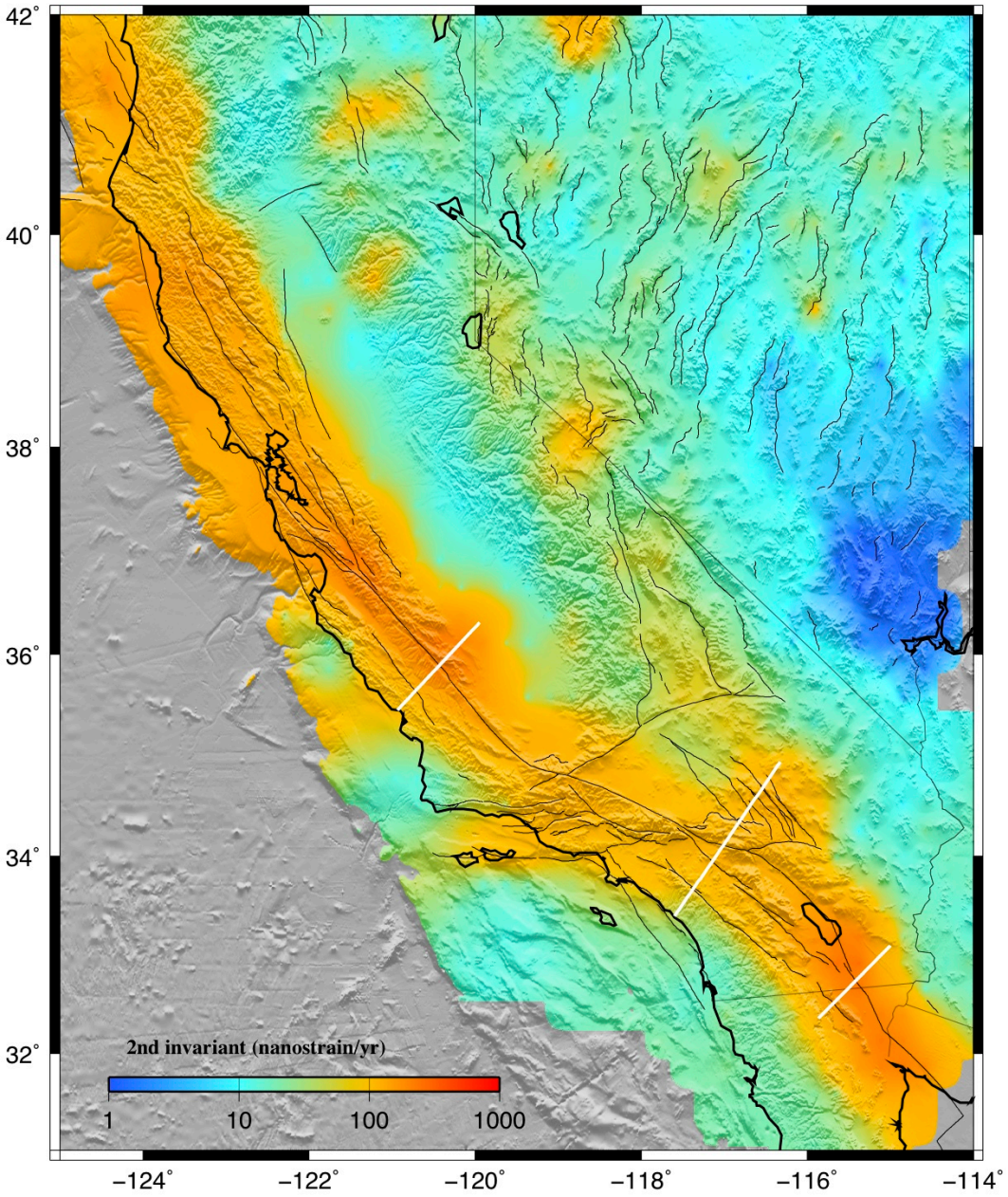

becker

082 ηs

Interpolated crustal strain rates based on the 20091130142023 releaseof the PBO GPS velocities, merged with the compilation by Kreemer andHammond (Geology, 2007). A high quality selection of data was used andprocessed via standard Generic Mapping Tools software (surface,grdfilter, grdgradient). The procedure follows that used in Platt etal. (EPSL, 2008), see that paper and Platt and Becker (submitted,2010; http://geodynamics.usc.edu/~becker/preprints/pb10.pdf)

fordetails.

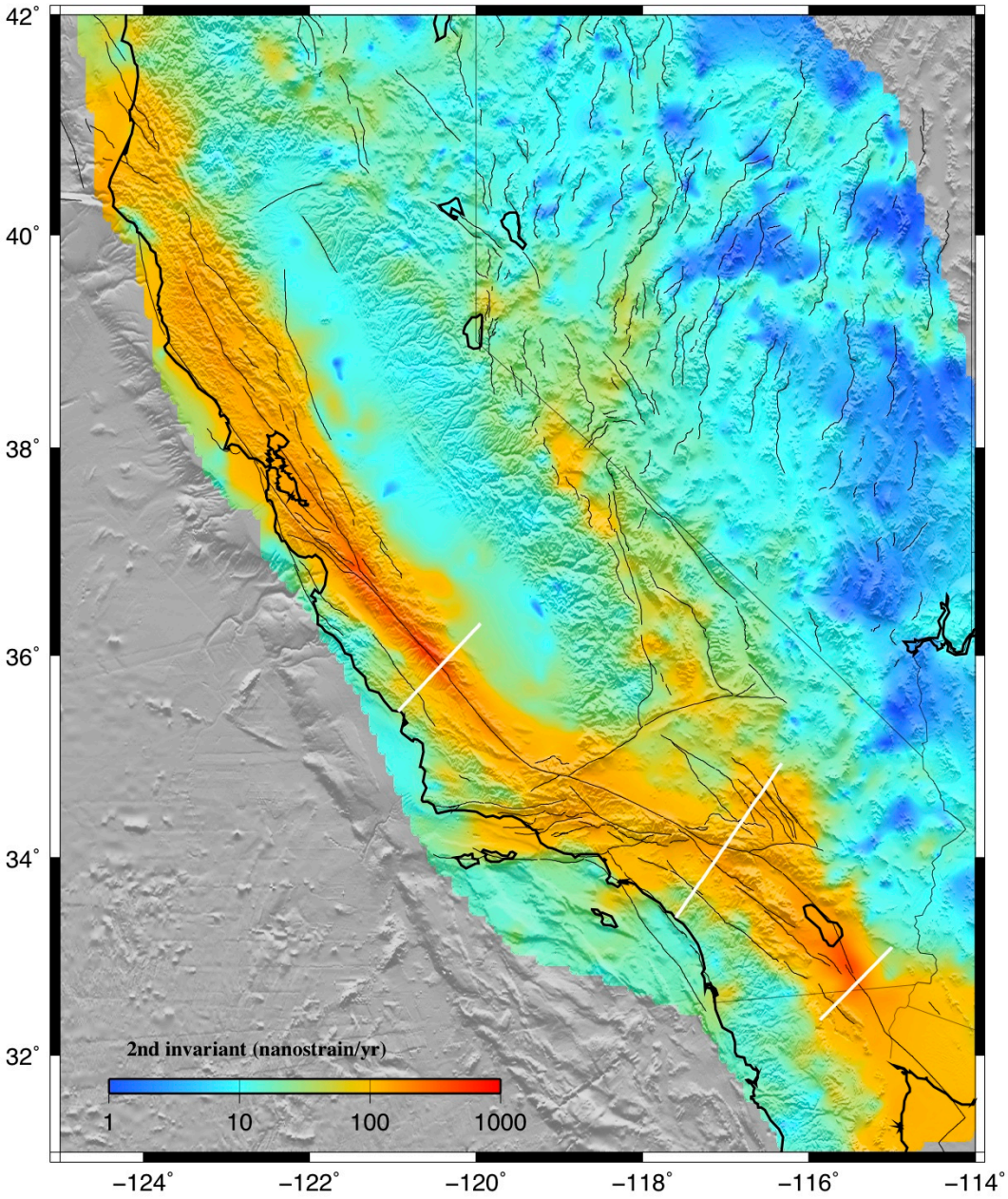

shen

086 ηs

Attached please find our data file. Interpolation is done using a weighting function†based on†azimuthal span and gaussian distance, and the decay distance constant is determined from a trade-off between the solution uncertainty and the weighting coefficient. Stations located in the 'shadow zone' behind the creeping section of the San Andreas are also screened out from the interpolation. The data file contains more items than you need, the ones relevant to your comparison are lat, lon, e11, e12, and e22.† '1' means east and '2' means north. You can discard the rest. Yuehua's solution submitted earlier was based on a slightly different approach, we will discuss the difference between that solution and†our current one in our presentation.† You may also enter both solutions in your comparisons if you like.

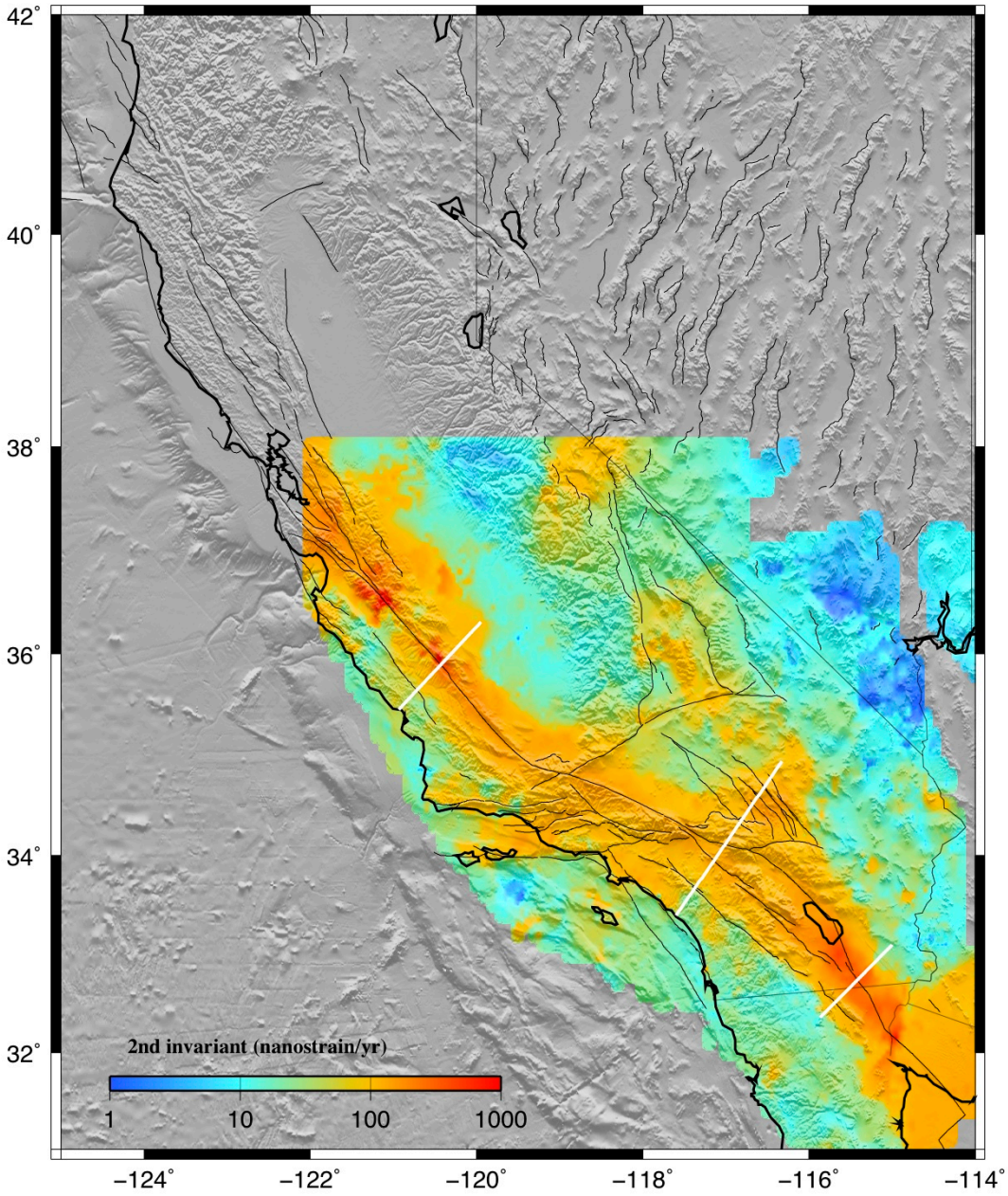

bormann_hammond 091 ηs

Jayne Bormann and Bill Hammond sent two velocity fields on a uniform grid constructed from their test exercise using CMM4. Hammond's code was used. Surface creep was not included and a uniform locking depth of 15 km was used.

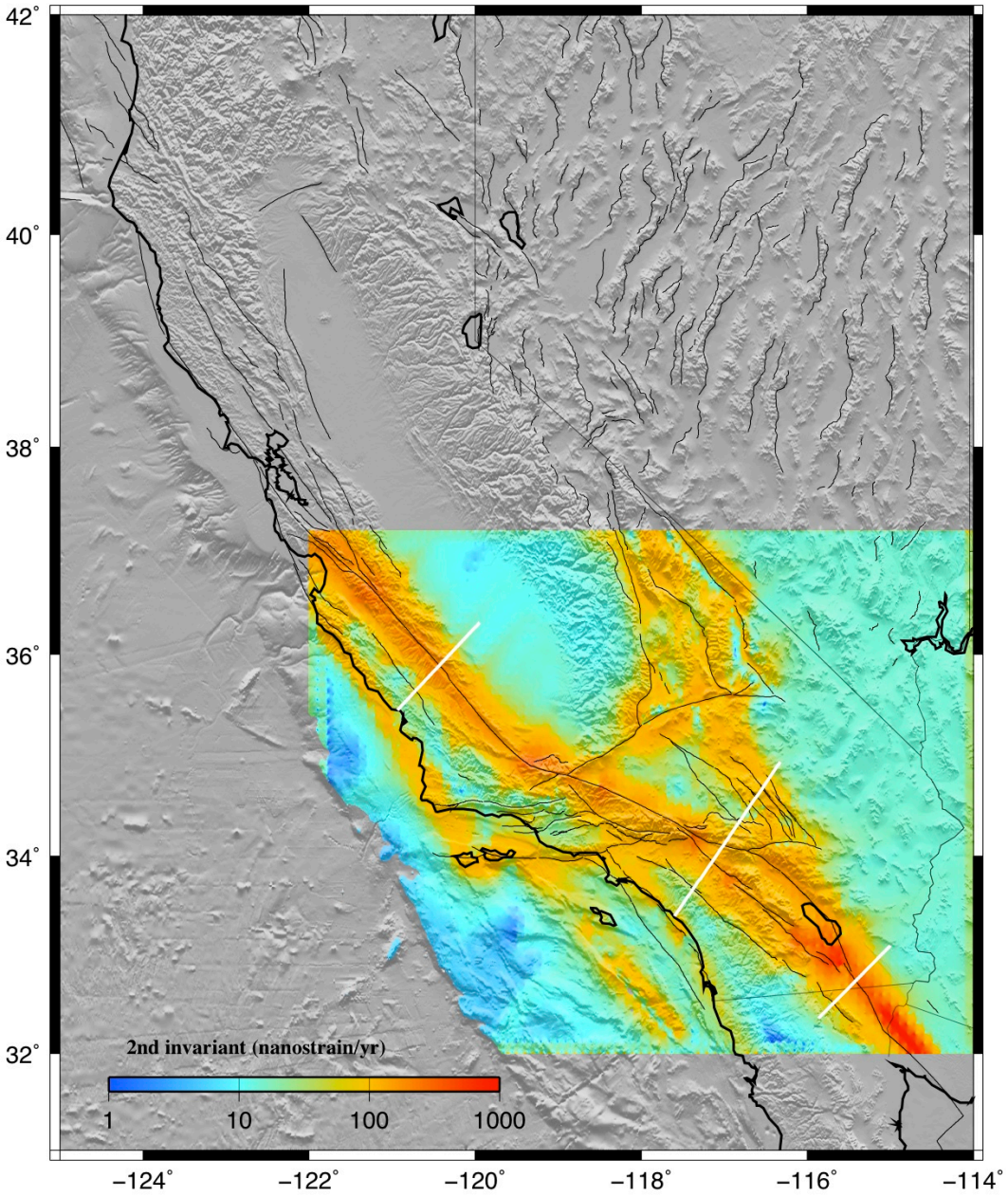

parsons

093 ηs

Tectonic stressing in California modeled from GPS observations Parsons,Tom Journal of Geophysical Research, Volume 111, Issue B3, CiteID B03407

What happens in the crust as a result of geodetically observed secular motions? In this paper we find out by distorting a finite element model of California using GPS-derived displacements. A complex model was constructed using spatially varying crustal thickness, geothermal gradient, topography, and creeping faults. GPS velocity observations were interpolated and extrapolated across the model and boundary condition areas, and the model was loaded according to 5-year displacements. Results map highest differential stressing rates in a 200-km-wide band along the Pacific-North American plate boundary, coinciding with regions of greatest seismic energy release. Away from the plate boundary, GPS-derived crustal strain reduces modeled differential stress in some places, suggesting that some crustal motions are related to topographic collapse. Calculated stressing rates can be resolved onto fault planes: useful for addressing fault interactions and necessary for calculating earthquake advances or delays. As an example, I examine seismic quiescence on the Garlock fault despite a calculated minimum 0.1-0.4 MPa static stress increase from the 1857 M~7.8 Fort Tejon earthquake. Results from finite element modeling show very low to negative secular Coulomb stress growth on the Garlock fault, suggesting that the stress state may have been too low for large earthquake triggering. Thus the Garlock fault may only be stressed by San Andreas fault slip, a loading pattern that could explain its erratic rupture history.

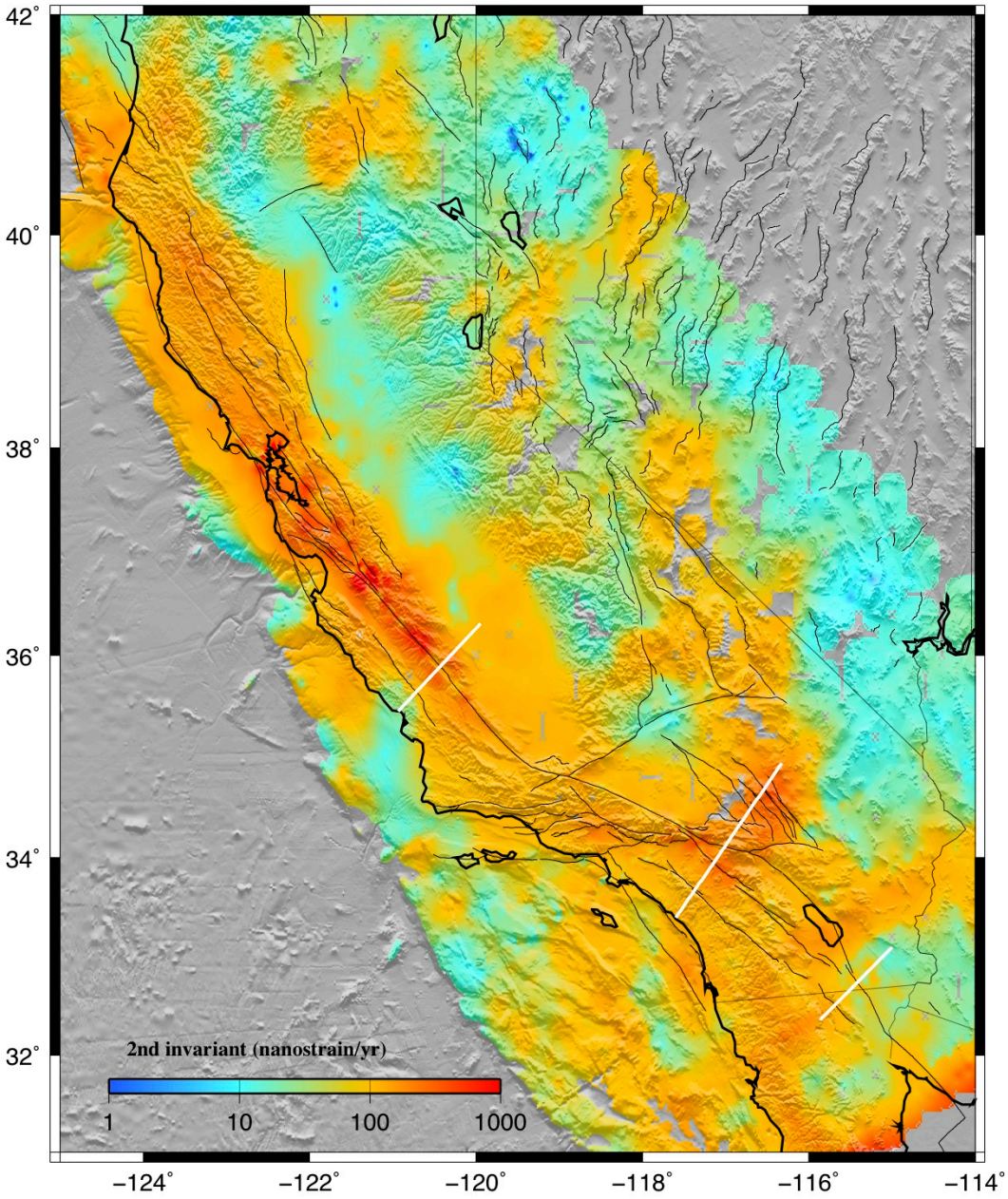

zeng

095 ηs

The GPS data for the western US are obtained from PBO velocity at UNAVCO site, Southern California Earthquake Center California Crustal Motion Map 1.0, McCaffrey et al. (2007) for Pacific Northwest, the GPS velocity field of Nevada and its surrounding area from the Nevada Geodetic Lab at the University of Nevada at Reno, and the GPS velocity field of the Wasatch-Front and the Yellowstone-Snake-River-River-Plain network from Bob Smith of University of Utah. These separate velocity fields are combined by adjusting their reference frames to make velocities match at collocated stations. I determined the Voronoi cells for this combined GPS stations and used their areas to weight the corresponding stations for inversion. I then interpolated those GPS observation into uniform grid point for the western US using the method of Wald (1998) and calculated the final strain rate map.

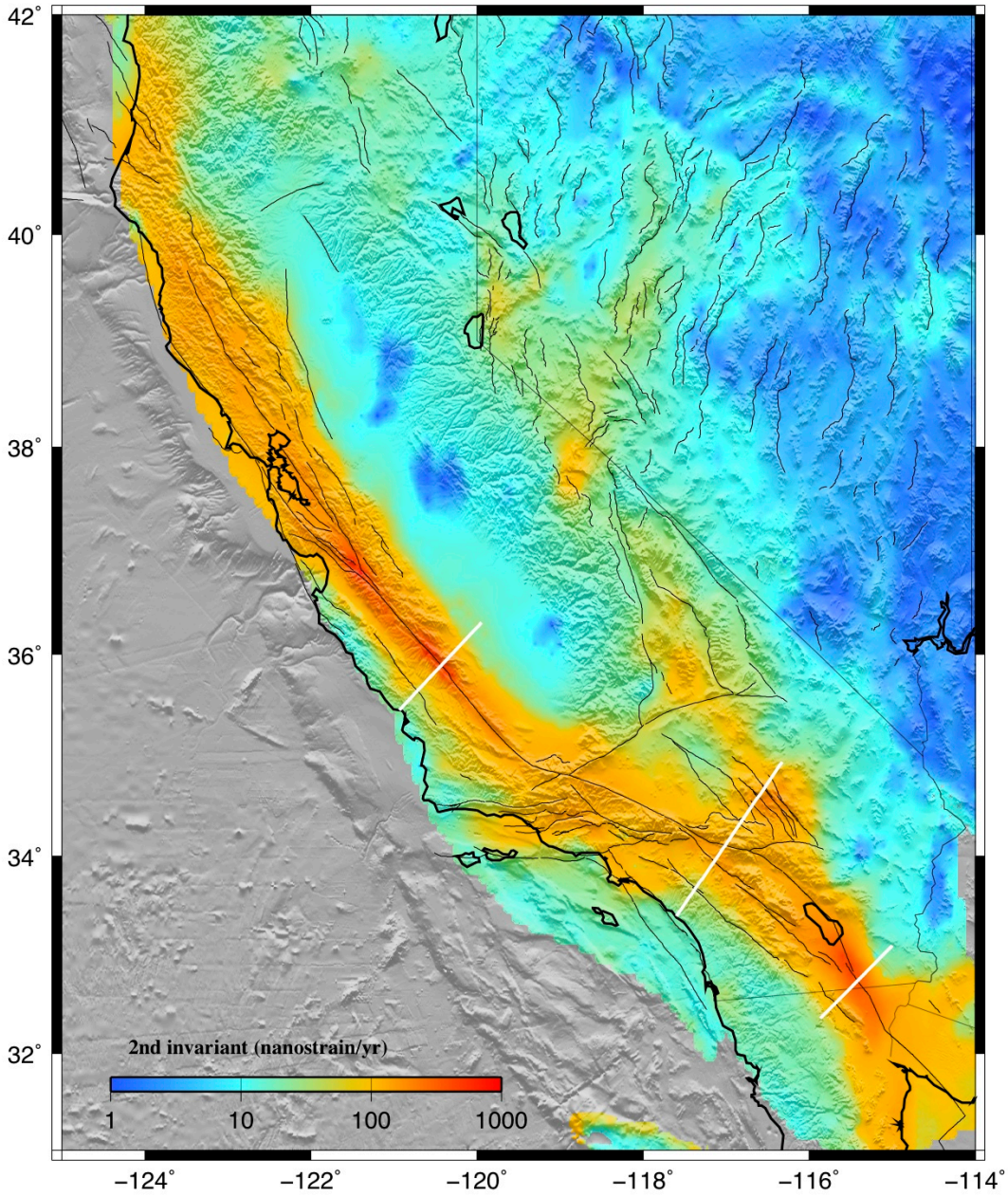

holt

111 ηs

What I do is use an anisotropic variance-covariance matrix for the strain rates. I do not build in fault slip rates, but I use the variance-covariance matrix to place a priori constraints on expected shear directions as well as some constraints on expected shear magntitudes. However, in the end the GPS velocities dictate the actual strain rates and styles of strain rate (where they are high, low, etc.). I am also limited by the finite-element grid, which is .1x.1 degree grid area spacing. It might be worthwhile to compare the solution I sent you with one obtained using fully isotropic uniform variances for all areas. That is, with an a priori expected strain rate distribution that is everywhere uniform. I can look into the reduced chi-squared misfit for both of these

cases.

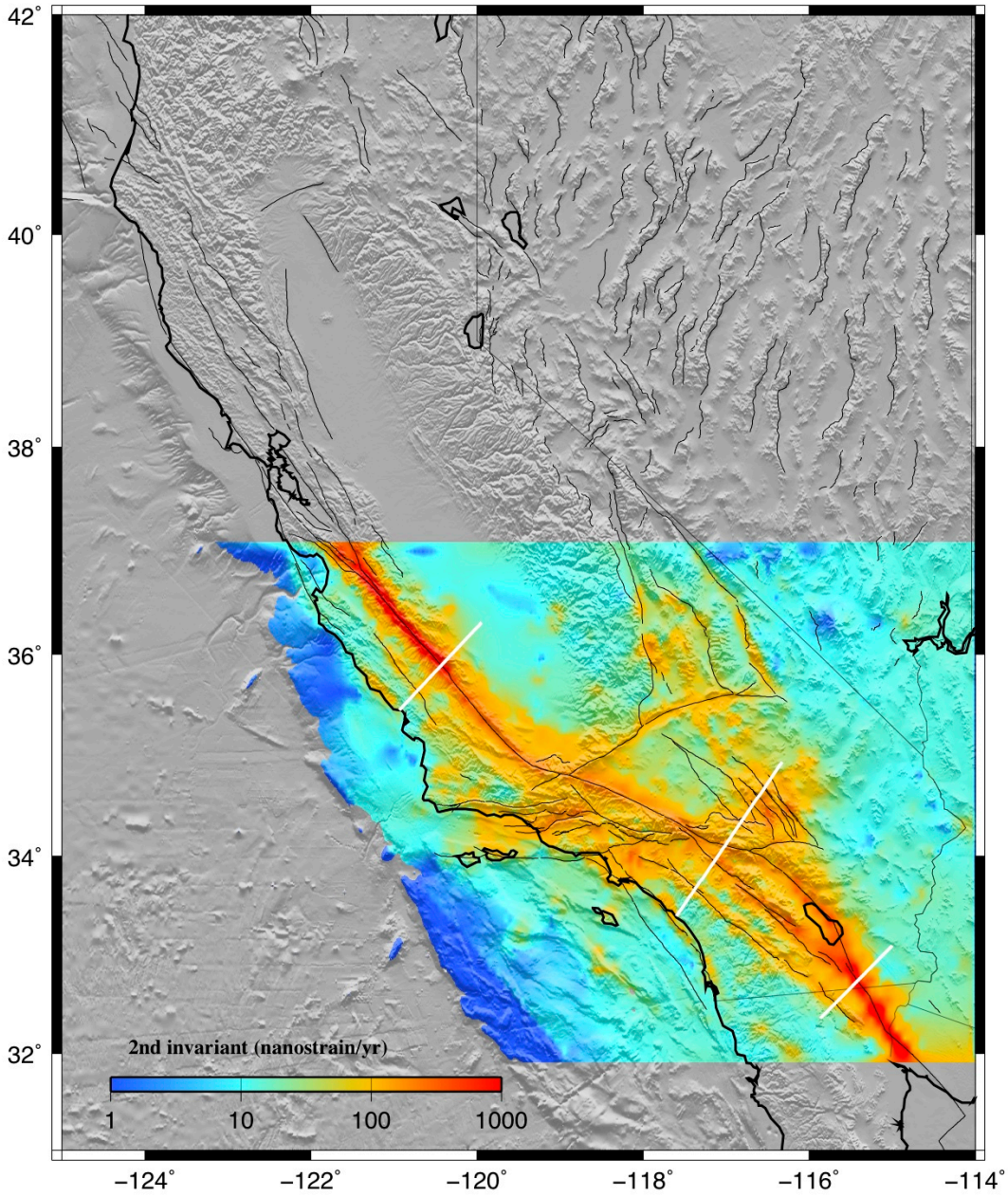

kreemer

114 ηs

Strain rate tensor model derived from fitting a continuous horizontal velocity field through GPS velocities [Kreemer et al, 2009]. 2053 GPS velocities were used, of which 854 from our own analysis of (semi-) continuous sites and 1199 from published campaign measurements (all transformed into the same reference frame). The model assumes that the deformation is accommodated continuously, and lateral variation in damping is applied to ensure that the reduced chi^2 fit between observed and modeled velocities is ~1.0 for subregions.

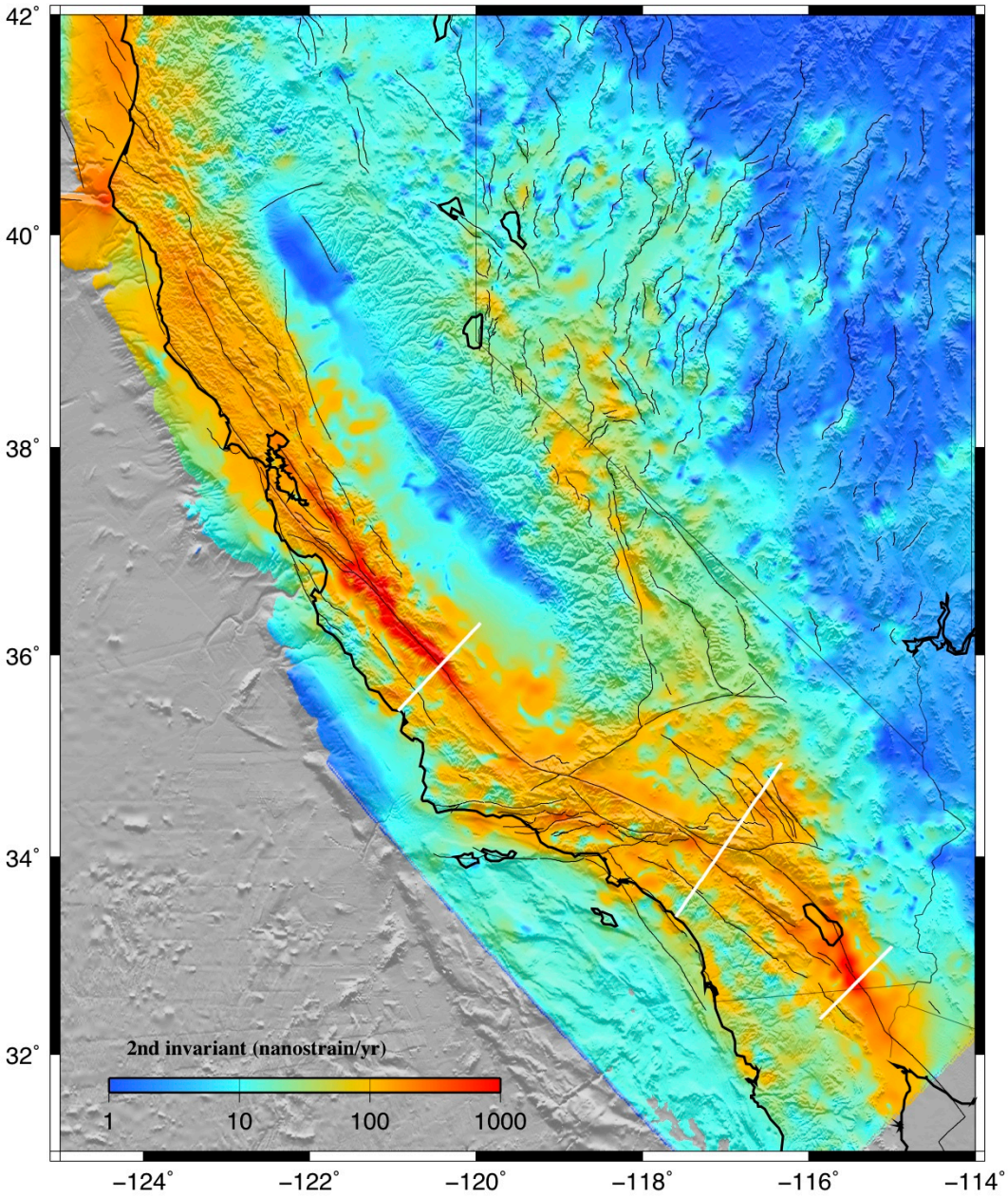

smith_konter

123 ηs

Strain rate derived from a dislocation model of the San Andreas Fault system [Smith-Konter and Sandwell, GRL, 2009]. 610 GPS velocity vectors were used to develop the model. The model consists of an elastic plate over a visco-elastic half space at 1 km horizontal resolution. Deep slip occurs on 41 major fault segments where rate is largely derived from geological studies. The locking depth is varied along each fault segment to provide a best fit to the GPS data. The model is fully 3-D and the vertical component of the GPS vectors is also used in the adjustment. An additional velocity model was developed by gridding the residuals to the GPS data using the GMT surface program with a tension of 0.35. This was added to the dislocation model.

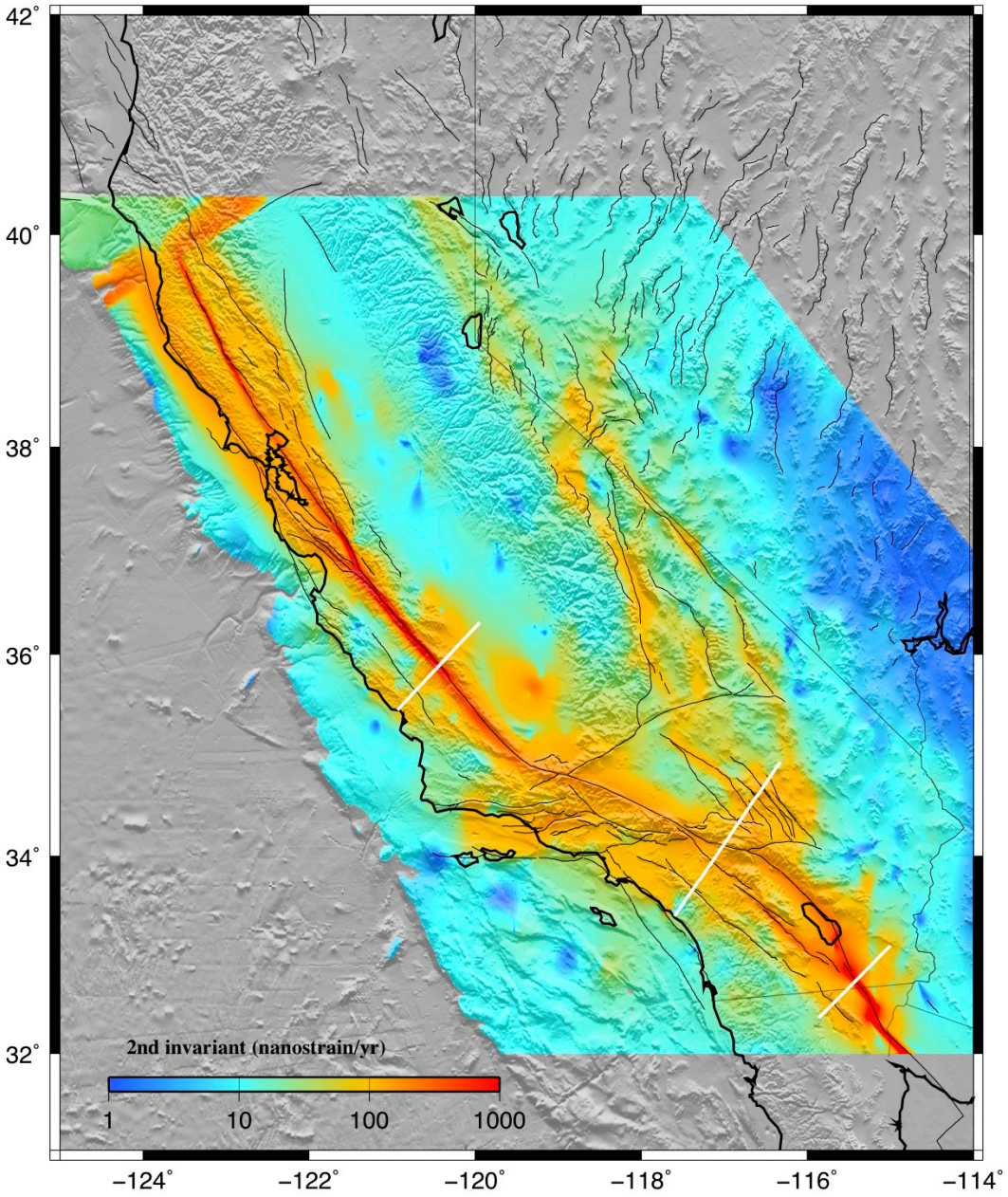

hackl

135 ηs

M. Hackl, R. Malservisi, and S. Wdowinski, Strain rate patterns from dense GPS networks, Nat. Hazards Earth Syst. Sci., 9, 1177ñ1187, 2009

Here we present a method to obtain the full continuous strain rate tensor from dense GPS networks. The tensorial analysis provides different aspects of deformation, such as the maximum shear strain rate, including its direction, and the dilatation strain rate. These parameters are suitable to characterize the mech- anism of the current deformation. Using the velocity fields provided by SCEC and UNAVCO, we were able to localize major active faults in Southern California and to characterize them in terms of faulting mechanism. We also show that the large seismic events that occurred recently in the study region highly contaminate the measured velocity field that appears to be strongly affected by transient postseismic deformation.

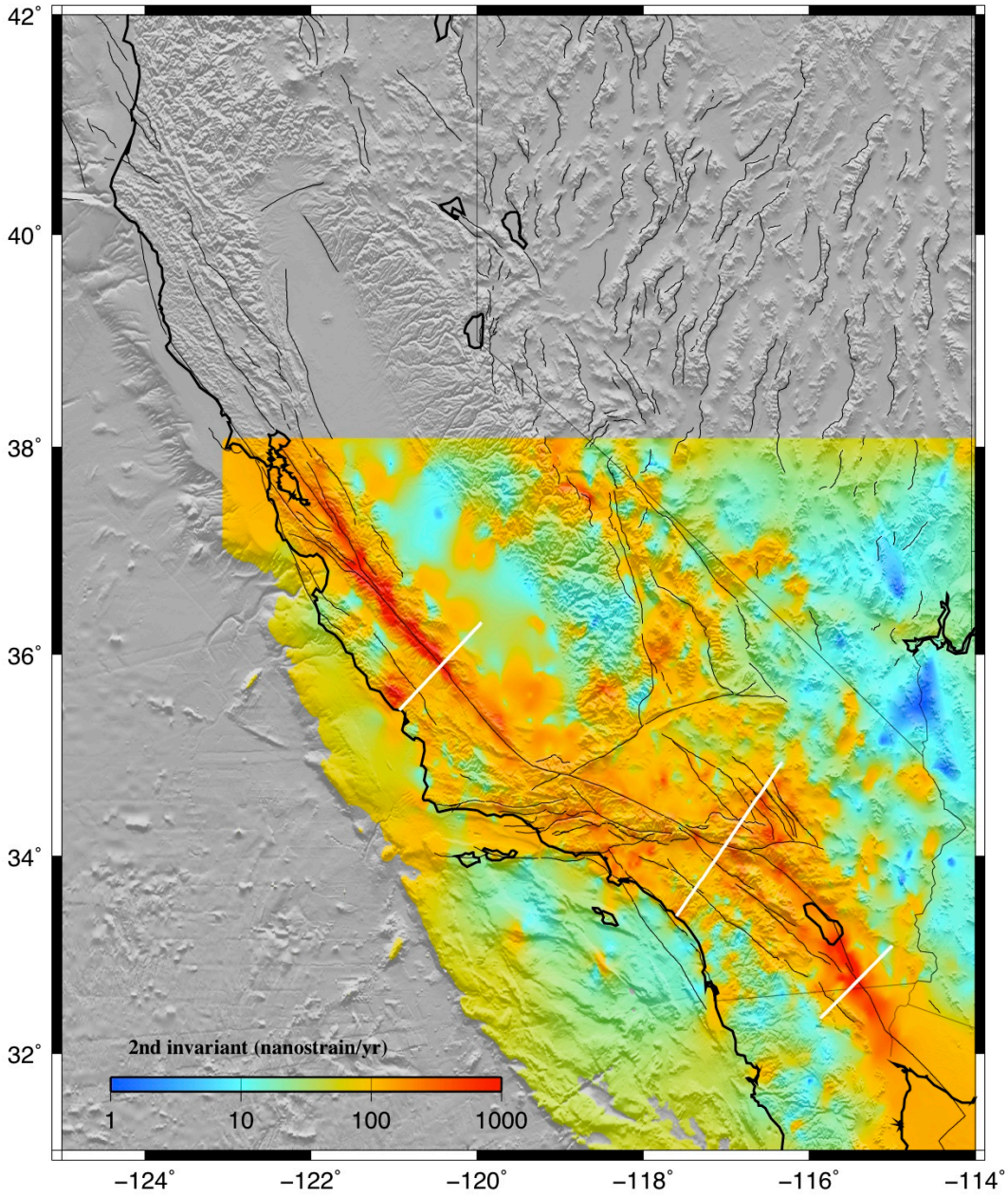

harvard

147 ηs

The strains are calculated analytically using elastic dislocation theory in a homogeneous elastic halfspace. The model is subset of a western US block model geodetically constrained by a combination of the SCEC CMM 3.0, McClusky ECSZ, Hammond Walker Lane, McCaffrey PNW, d'Allessio Bay Area, and PBO velocity fields. These are combined by minimizing residuals (6-parameter) at collocated stations. In southern California the block geometry is based on and the Plesch et al., CFM-R and features dipping faults in the greater Los Angeles regions which end up producing some intricate strain rate patterns. The model features fully coupled (locked from the surface to some locking depth) faults everywhere except for Parkfield, the SAF just north, and the Cascadia subduction zone. For Parkfield and Cascadia we solve for smoothly varying slip on surfaces parameterized using triangular dislocation elements.

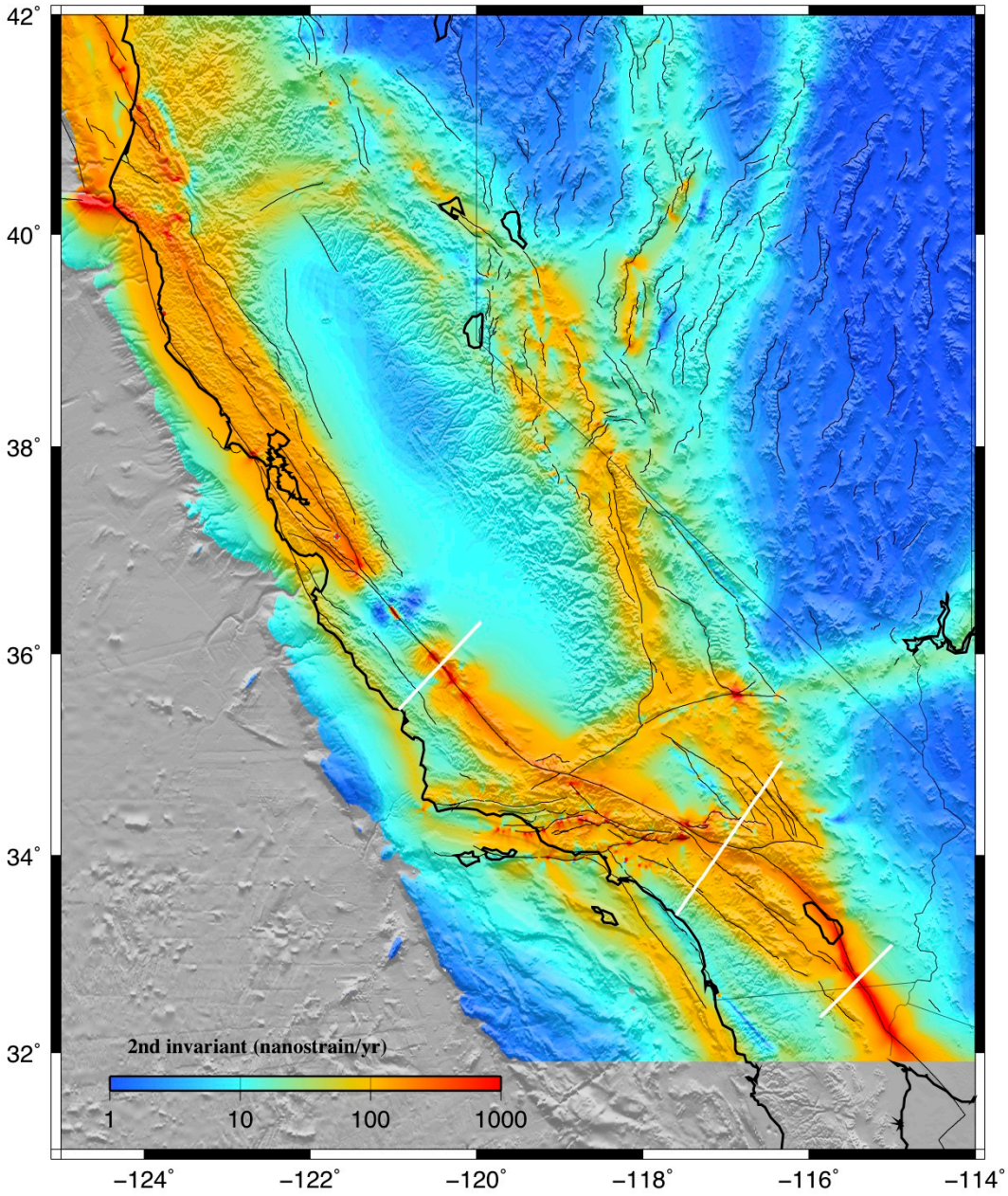

mccaffrey

147 ηs

Model of horizontal surface velocities (converted to strain) for the western United States. While there are many ways to go about doing this, here we have chosen to generate a geologic block model, constrained by observations from geodesy, seismology and geology. The parameters of the block model are constrained by non-linear least-squares inversion. The locking depth is set to 10 km for segments where locking depth is not well constrained by GPS. The model is used to predict surface velocity on a uniform grid at 0.02 degree spacing. Grids were filtered at 0.5 gain at 10 km wavelength.

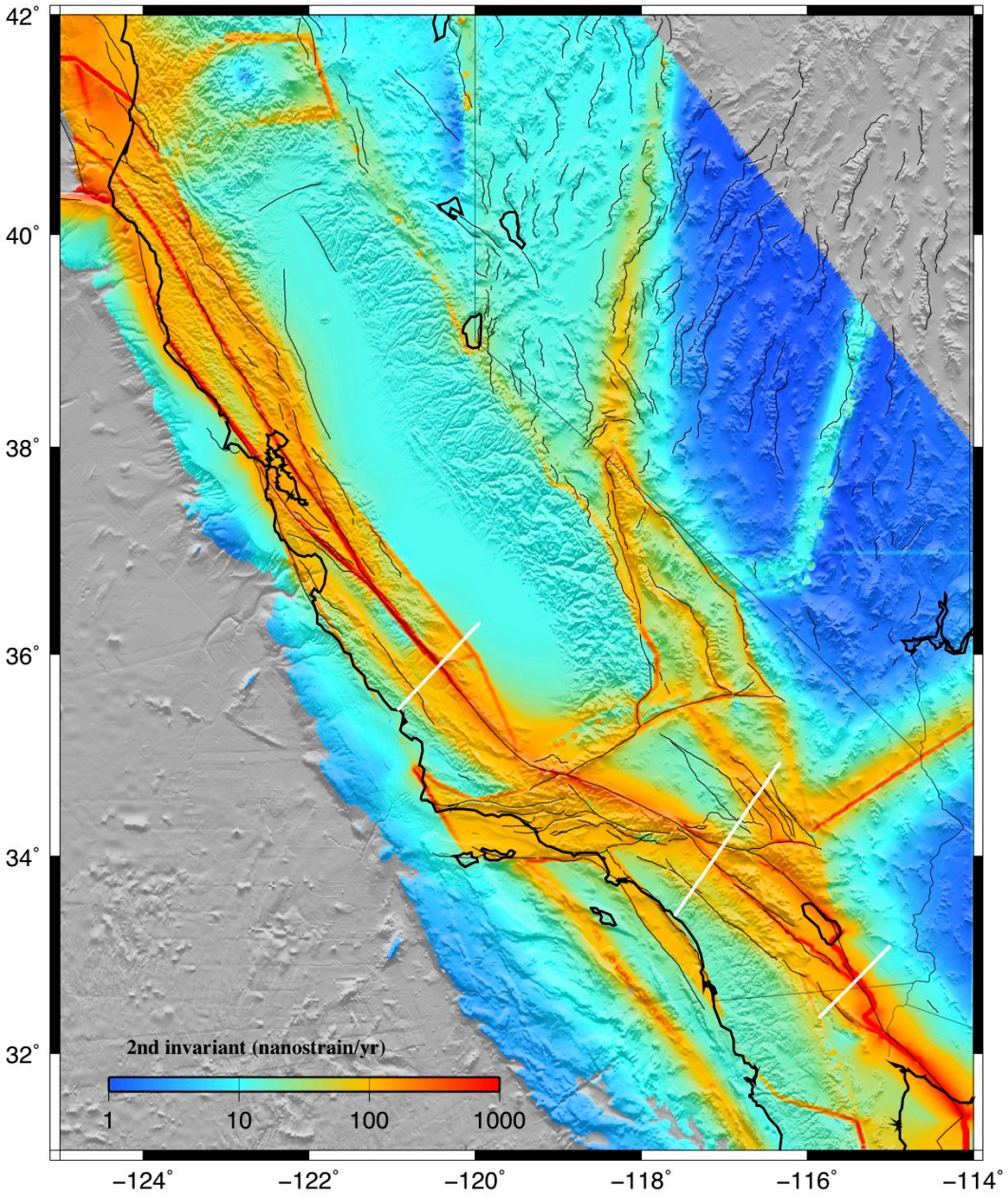

bird

147 ηs

Attached are my interseismic strain-rate results for two NeoKinema models of the southern California comparison test exercise:

NeoKinema_composite_interseismic_strain_rate.zip
is my best/preferred composite model, using both the GPS rates provided and "my own" [Bird, 2007, 2009] geologic offset rates.

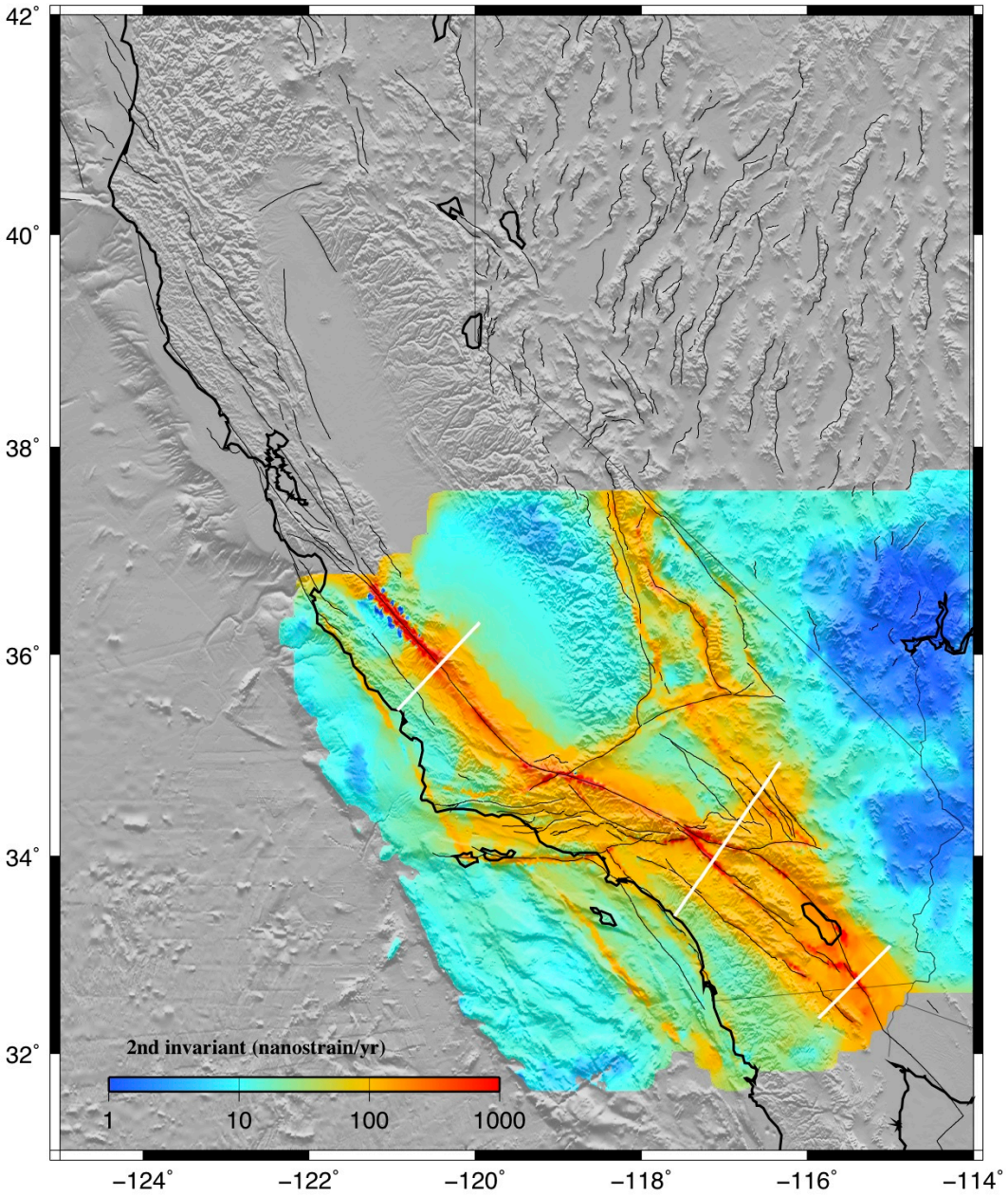

Reconciling Deformation/Stressing Rate Models

Community Stress Workshop
May 29, 2013

Assumptions:

- strain rate can be converted to stress rate using some rheology
- surface stress rate can be downward continued to seismogenic depth

Comparison of 17 strain rate models

Selection of 5 similar models

Coherence analysis of 4 models to establish spatial resolution

Comparison of 4 models with Yang EQ orientations

Where do we go from here?

Imperial array

High density campaign GPS measurements across the Imperial fault provide the data needed to estimate the strain rate [Lyons et al., 2002]. The best-fit 2-D dislocation model has a velocity V_o of 40 mm/yr and a locking depth D of 6 km (upper plot). The derivative of this velocity profile provides the shear strain rate (lower plot). The peak strain rate is given by

$$\dot{\varepsilon} = \frac{V}{\pi D}$$

which in this case has a value of 2120 nanostrain/yr.

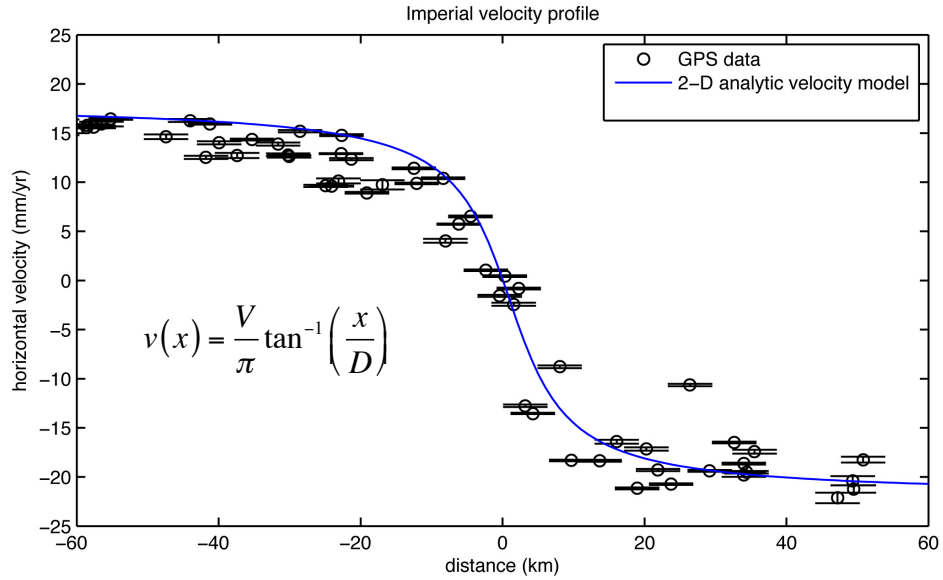

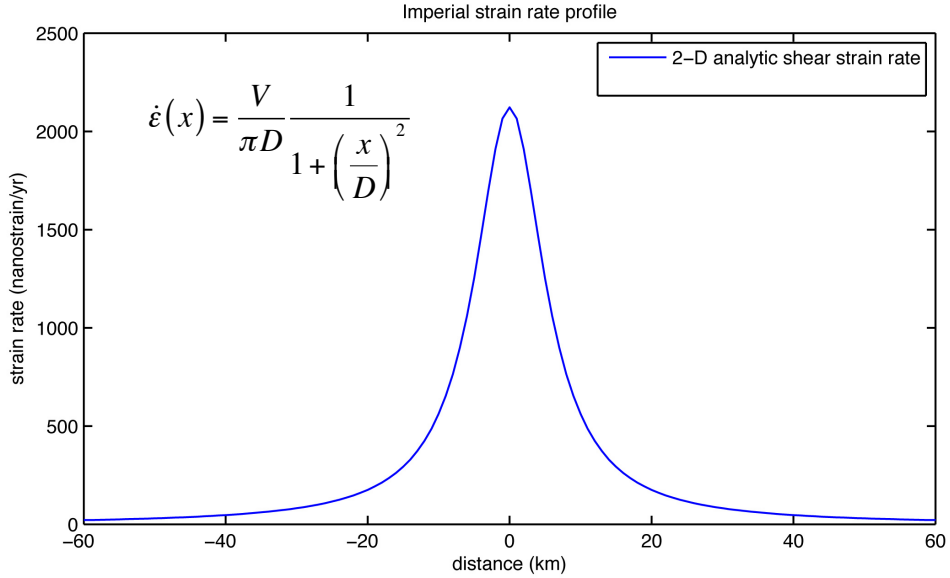

Carrizo GPS data

Earthquake Cycle Exercise, April, 2010.

“Participants were given a GPS velocity profile, that is, the fault-parallel velocity, one-sigma error, and distance to the fault for 64 GPS sites (Figure 10). The data were from the San Andreas Fault at the Carrizo Plain, though this was not mentioned in the exercise. Participants were asked to devise models that could explain the velocity profile.

Elastic dislocation models, including those with a dipping fault and elastic heterogeneities, gave a slip rate of 33 to 35 mm/yr and a locking depth of 17 to 19 km.”

Using V=35 and D=17 and the peak strain rate is 790 nanostrain/yr.

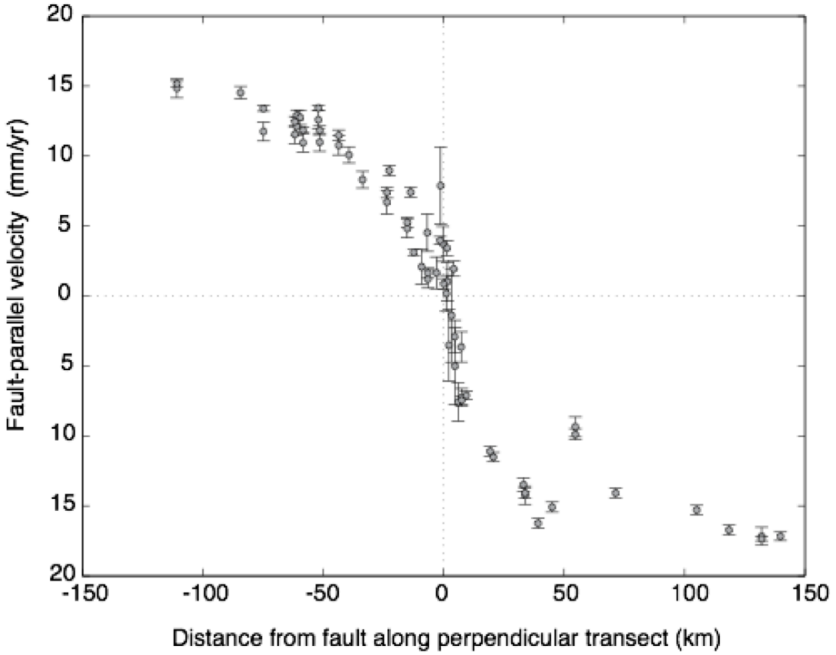

	elastic	viscoelastic	“believable” viscoelastic	viscoelastic with fault creep	“believable”viscoelastic with fault creep
Vo (mm/yr)	33.5 - 37	30-60	33-35 (36-40)	35-45	33-35 (35-40)
Zl (km)	16 - 19	6 to 25	16-18 (20-25)	5 -19	10 -15(10)
stress rate (kPa/yr)	25	18-30	25-26	23-25	20-25

Strain rate profiles from all 17 models.

Comapred with best-fit 2-D Savage model

12 of the 17 models have unrealistic low strain rate

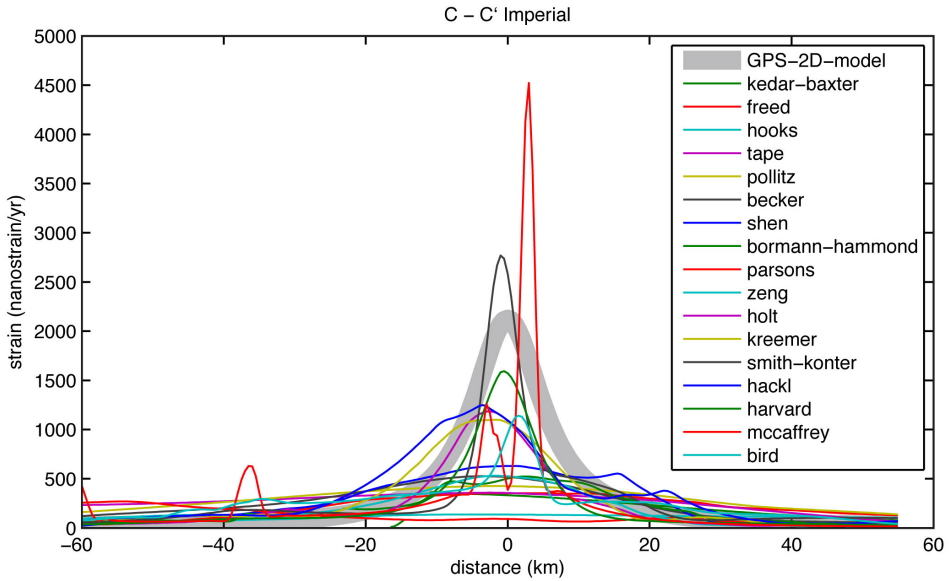

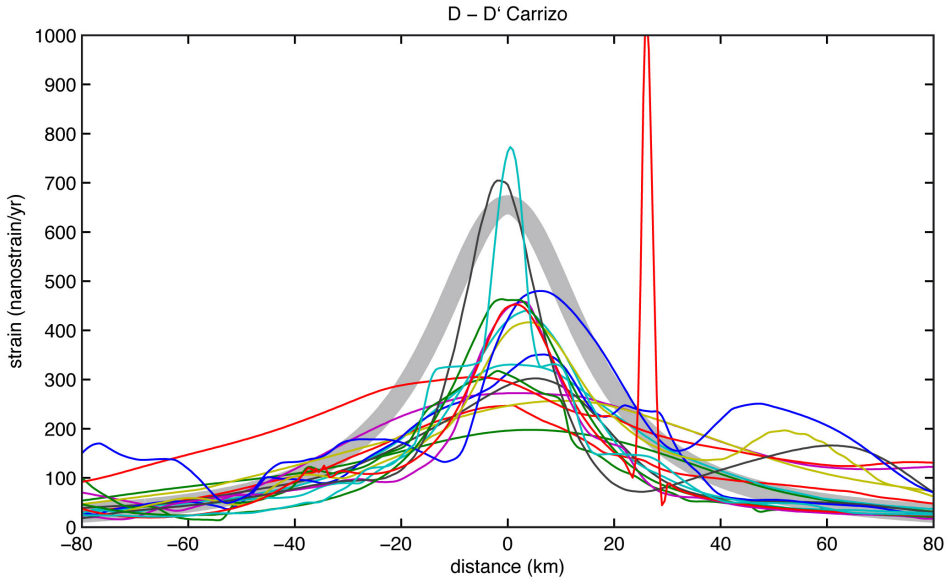

Strain rate profiles from 5 best models.

Comapred with best-fit 2-D Savage model

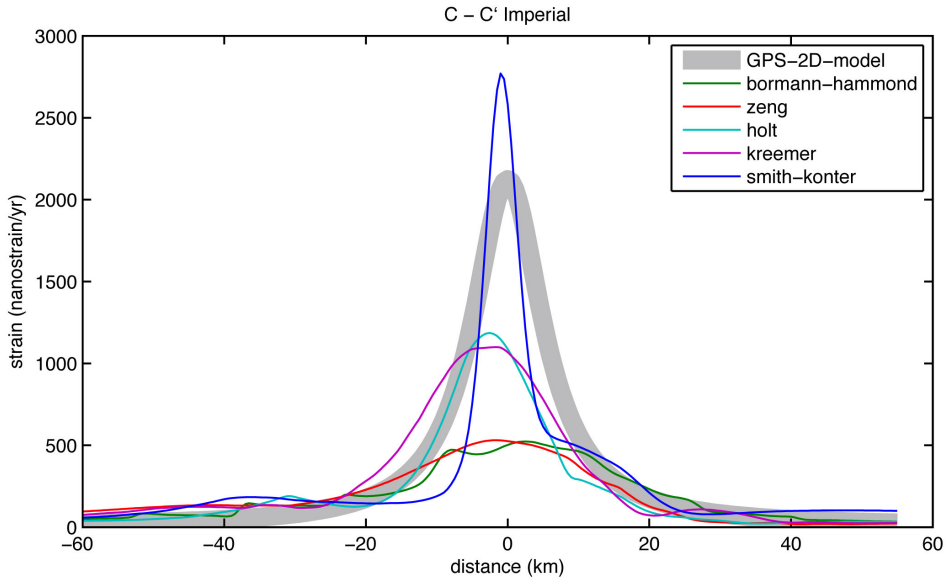

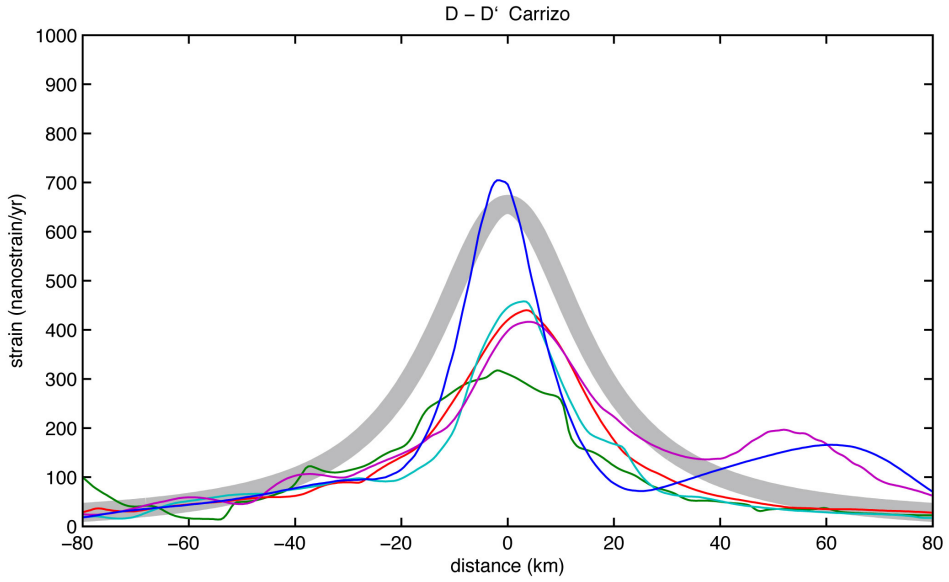

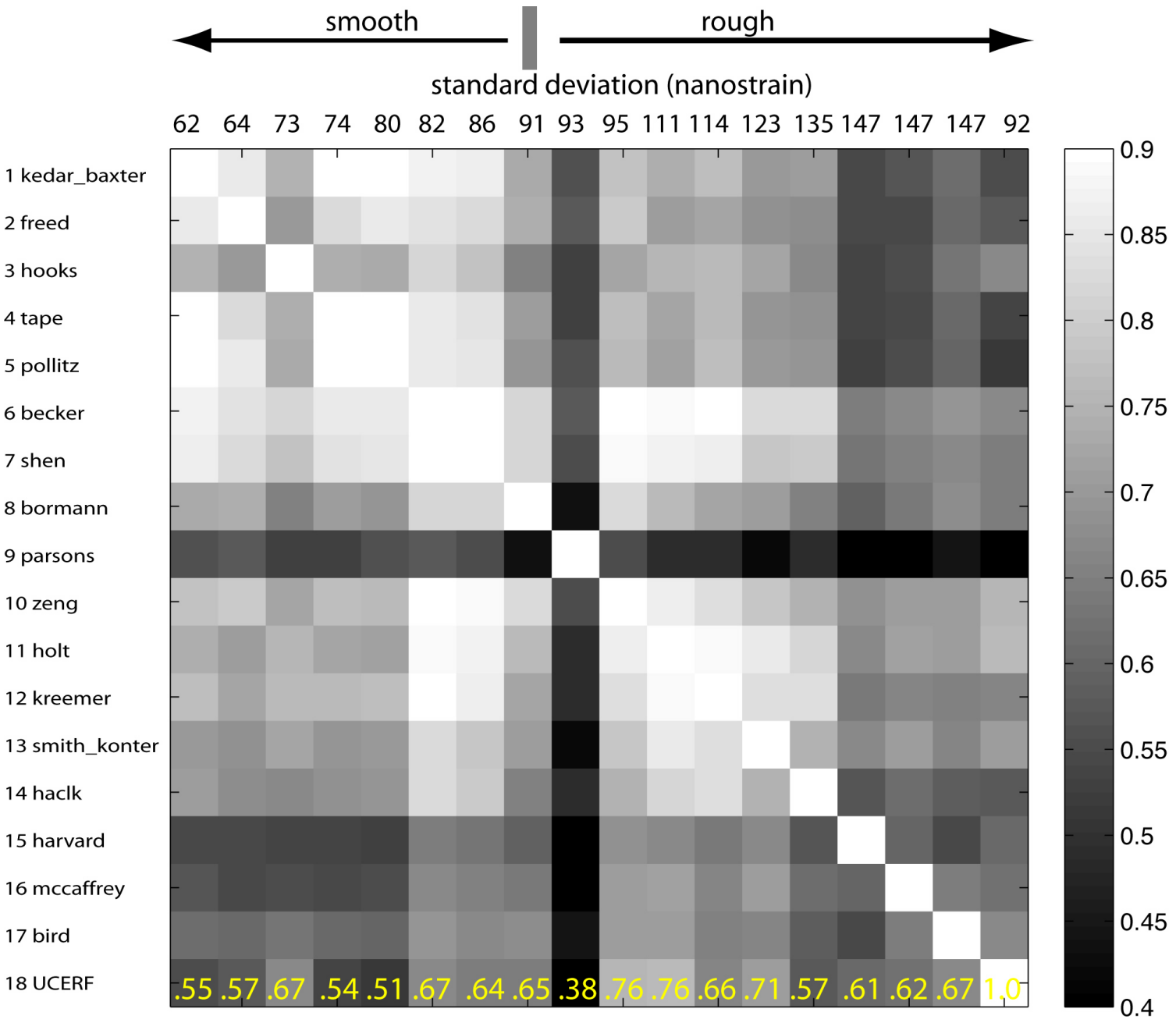
smooth
rough
standard deviation (nanostrain)
62 64 73 74 80 82 86 91 93 95 111 114 123 135 147 147 147 92
1 kedar_baxter
2 freed
3 hooks
4 tape
5 pollitz
6 becker
7 shen
8 bormann
9 parsons
10 zeng
11 holt
12 kreemer
13 smith_konter
14 haclk
15 harvard
16 mccaffrey
17 bird
18 UCERF
.55 .57 .67 .54 .51 .67 .64 .65 .38 .76 .76 .66 .71 .57 .61 .62 .67 1.0
0.9
0.85
0.8
0.75
0.7
0.65
0.6
0.55
0.5
0.45
0.4

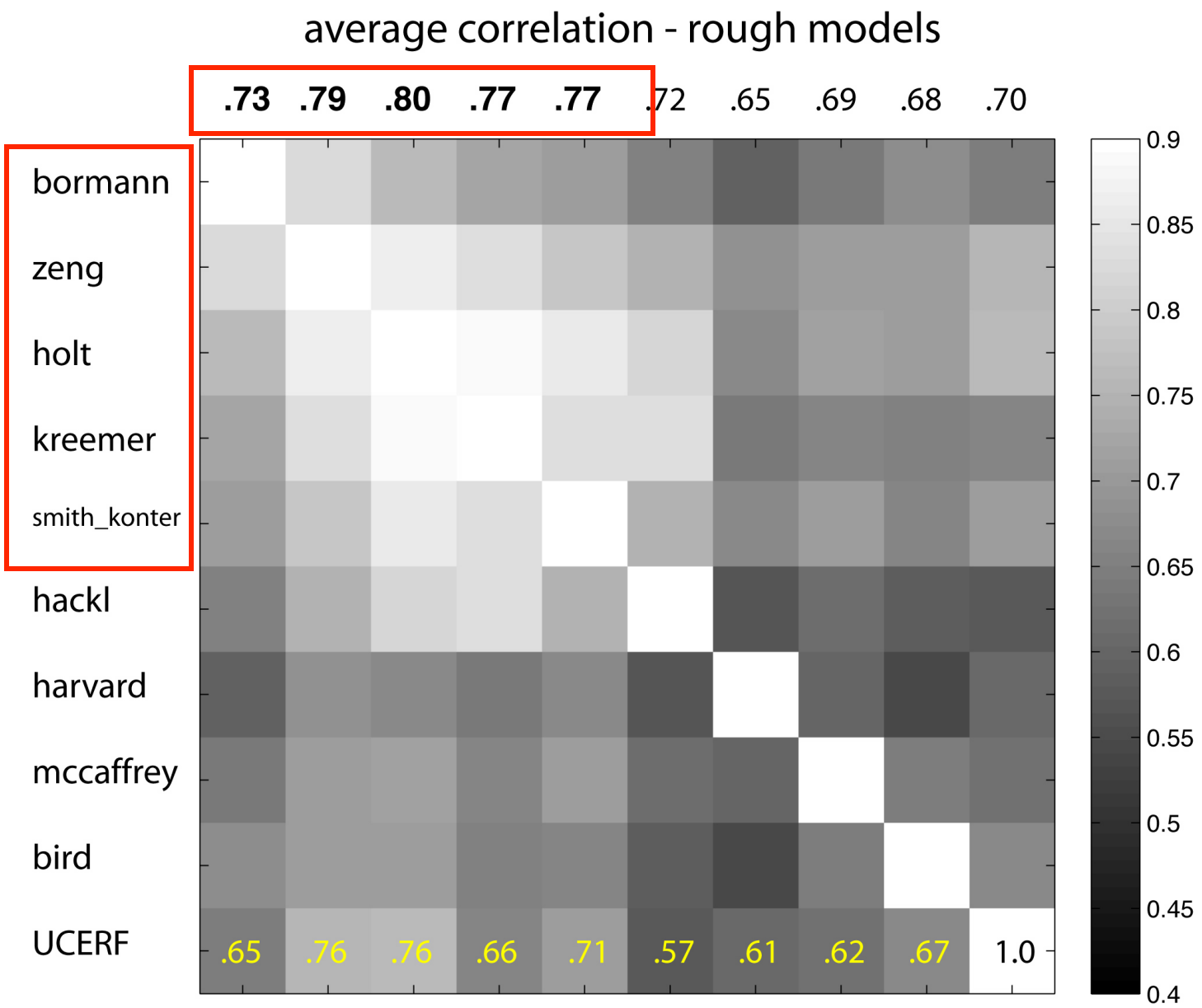
average correlation - rough models
.73 .79 .80 .77 .77 .72 .65 .69 .68 .70
bormann
zeng
holt
kreemer
smith_konter
hackl
harvard
mccaffrey
bird
UCERF
.65 .76 .76 .66 .71 .57 .61 .62 .67 1.0
0.9
0.85
0.8
0.75
0.7
0.65
0.6
0.55
0.5
0.45
0.4

average of 5 “best” models

mean

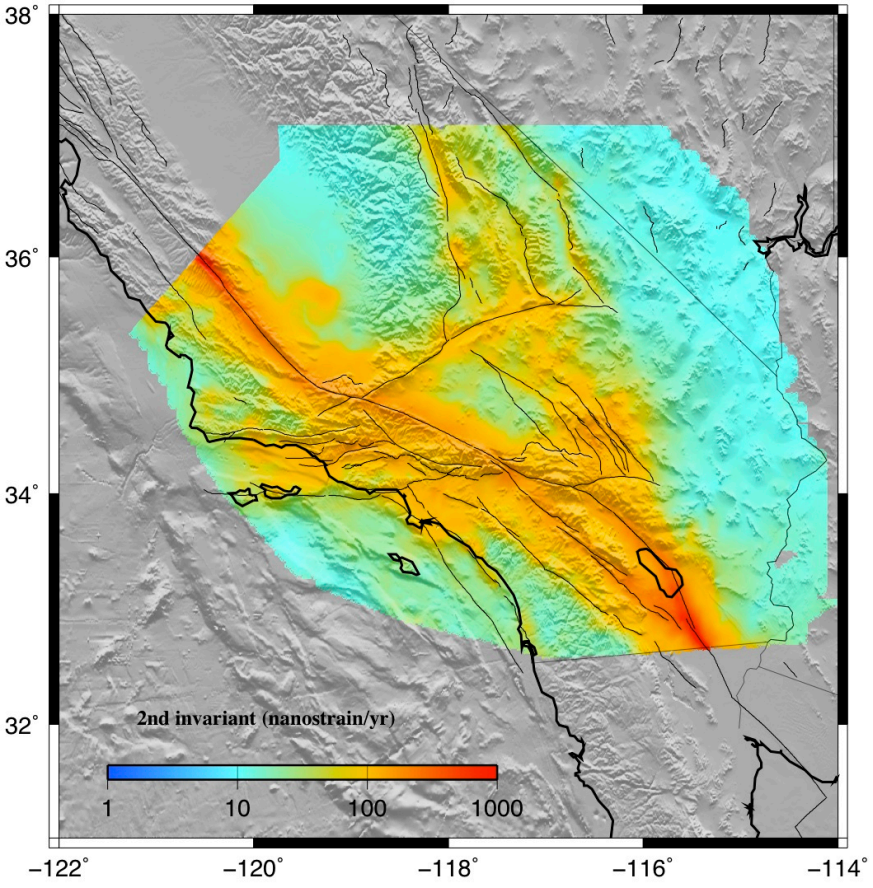

std of 5 “best” models

std

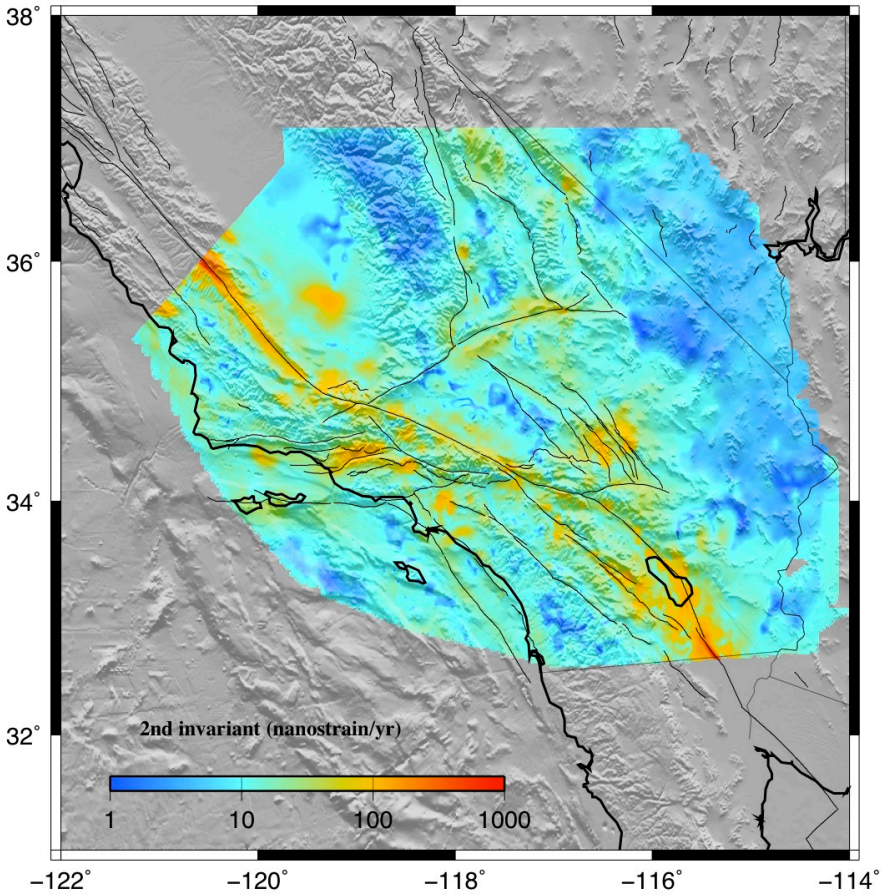

Reconciling Deformation/Stressing Rate Models

Community Stress Workshop
May 29, 2013

Assumptions:

- strain rate can be converted to stress rate using some rheology
- surface stress rate can be downward continued to seismogenic depth

Comparison of 17 strain rate models

Selection of 5 similar models

Coherence analysis of 4 models to establish spatial resolution

Comparison of 4 models with Yang EQ orientations

Where do we go from here?

Standard Deviations of 4 Block Models

Meade&Hager (2005); Smith-Konter and Sandwell (2009); McCaffrey (2005); Zeng(2010)

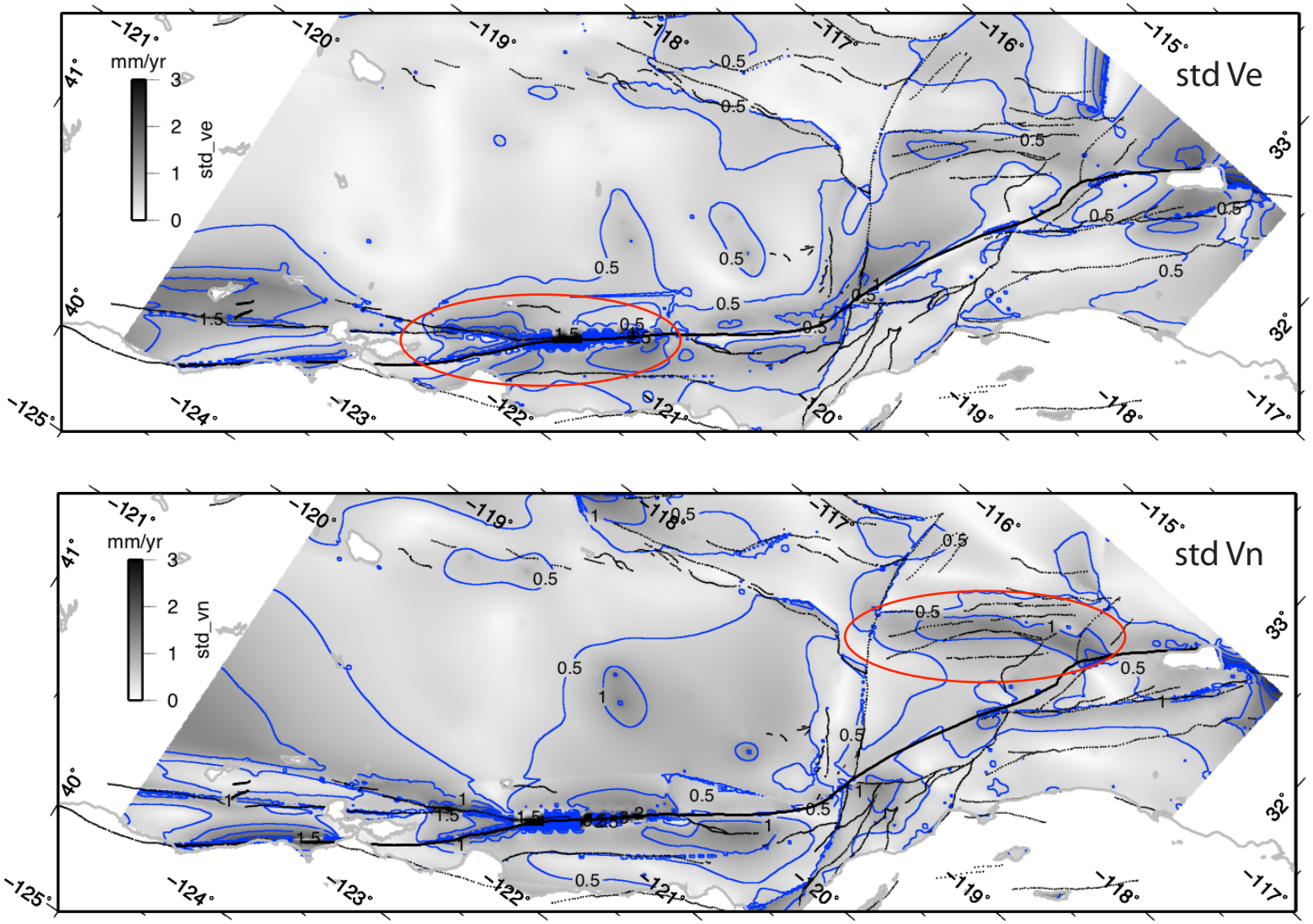

[Tong et al., 2102]

Coherence of 4 Block Models

Meade&Hager (2005); Smith-Konter and Sandwell (2009); McCaffrey (2005); Zeng(2010)

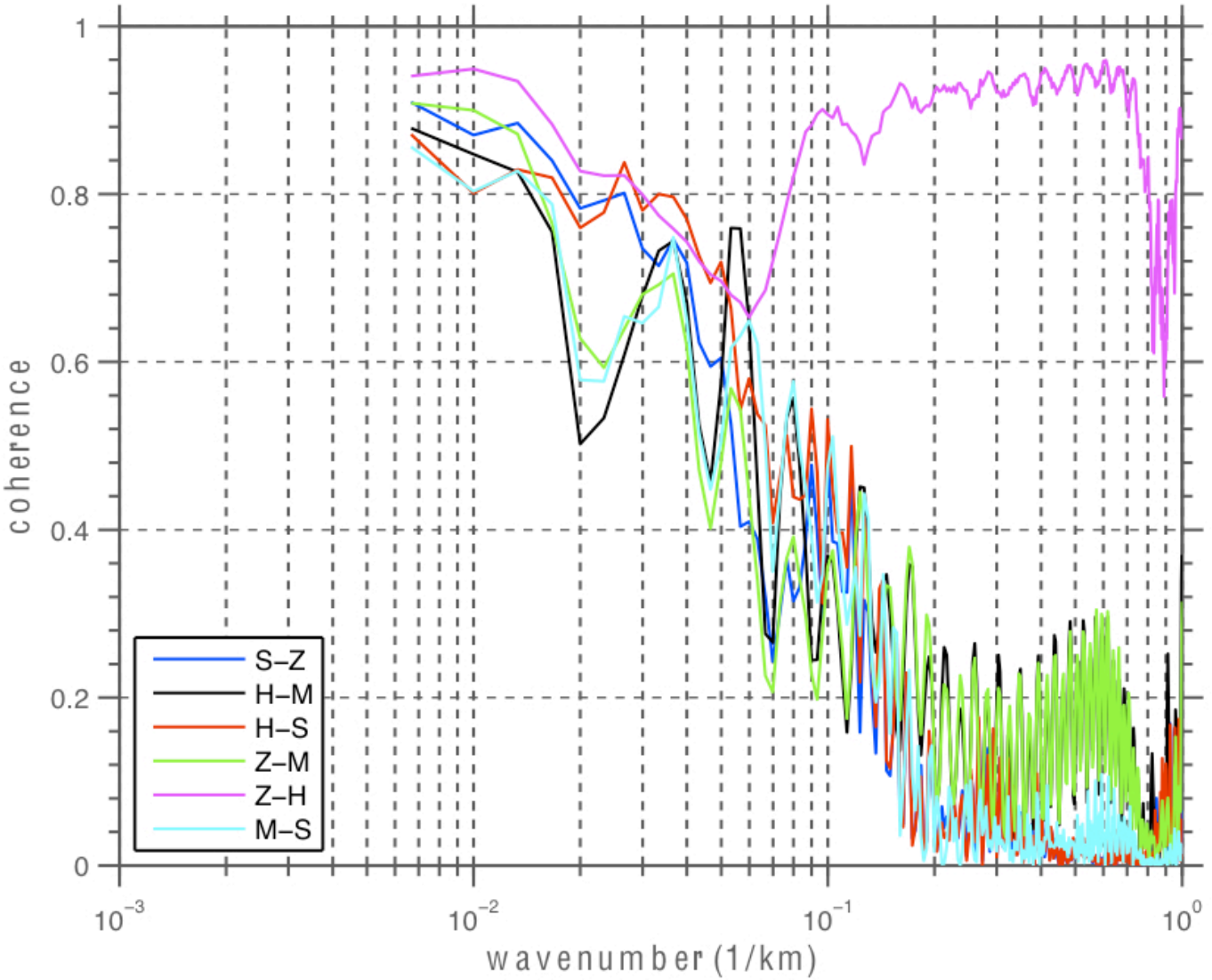

[Tong et al., 2102]

Coherence of 4 Block Models

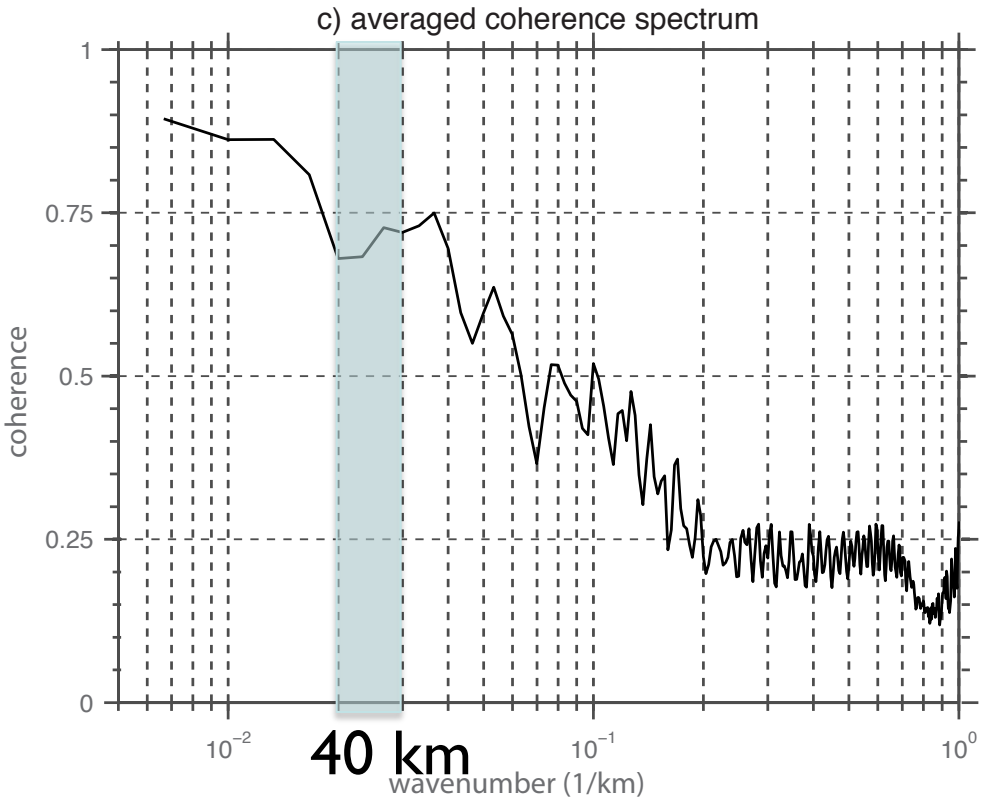

- GPS model are coherent at wavelength > 40 km.
- Models are incoherent at 5 km.

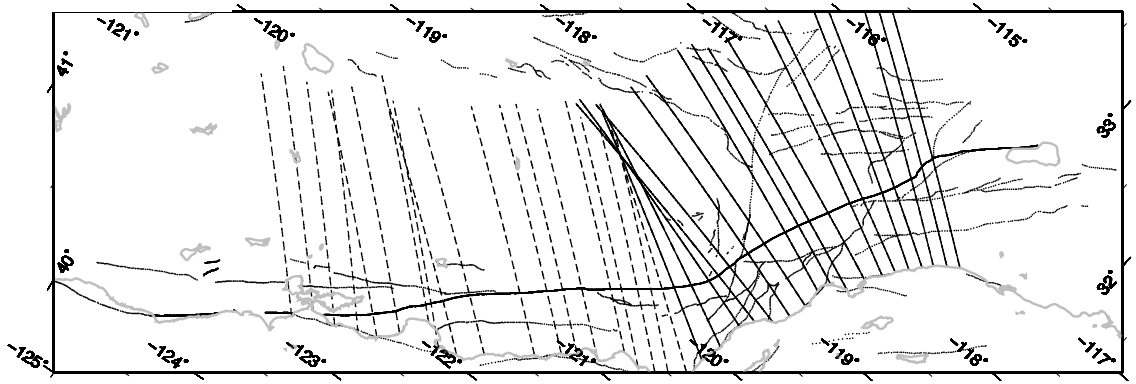

[Tong et al., 2102]

bormann_hammond

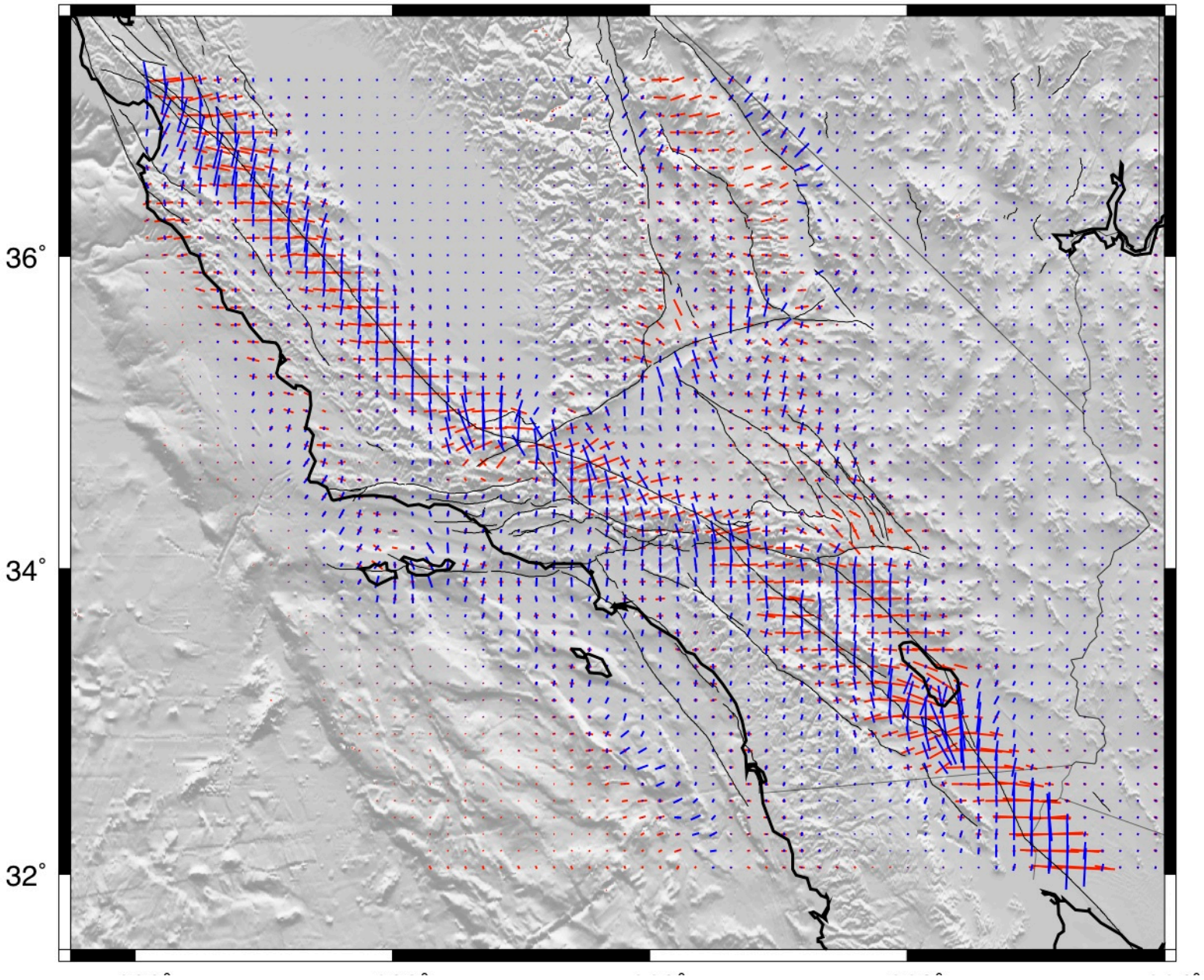

zeng

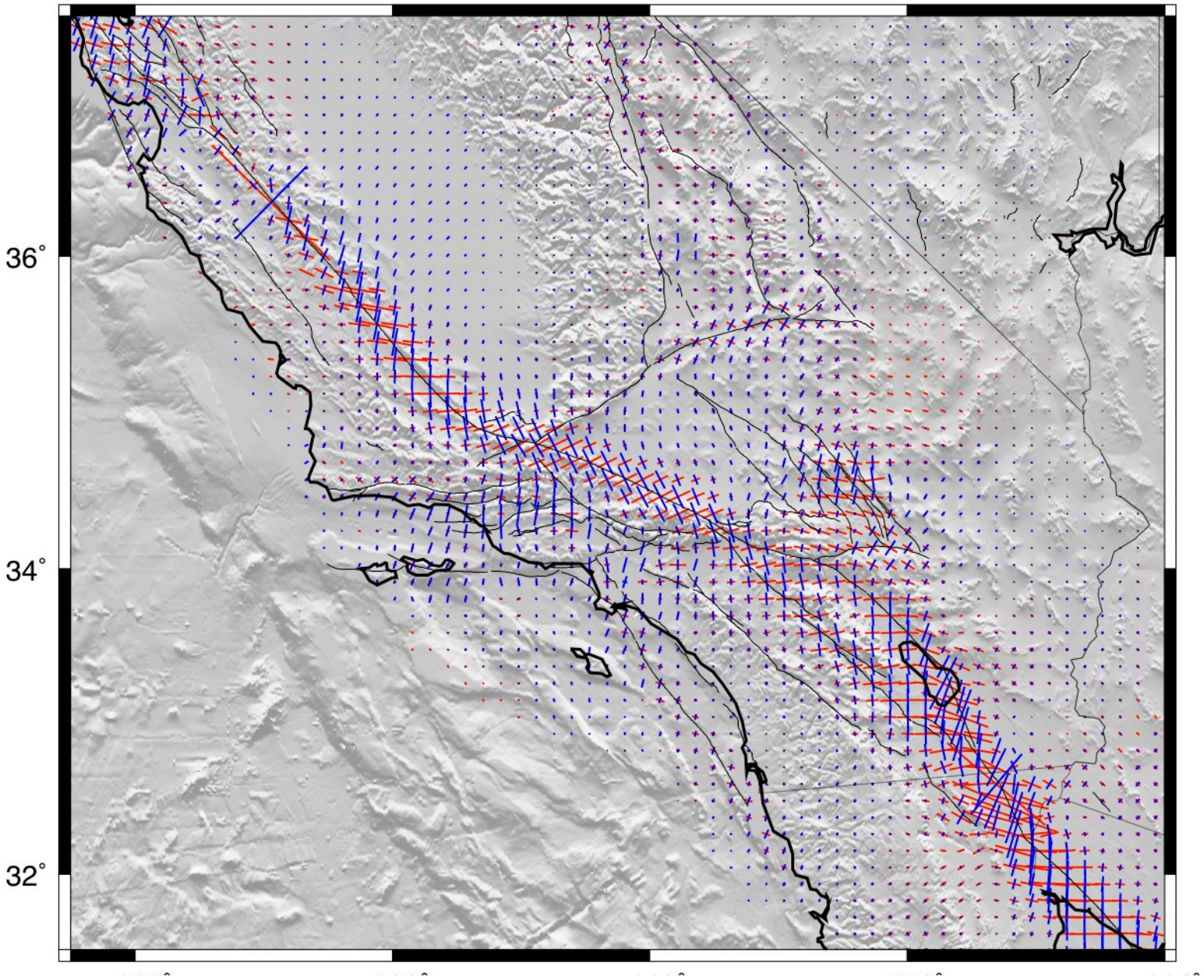

holt

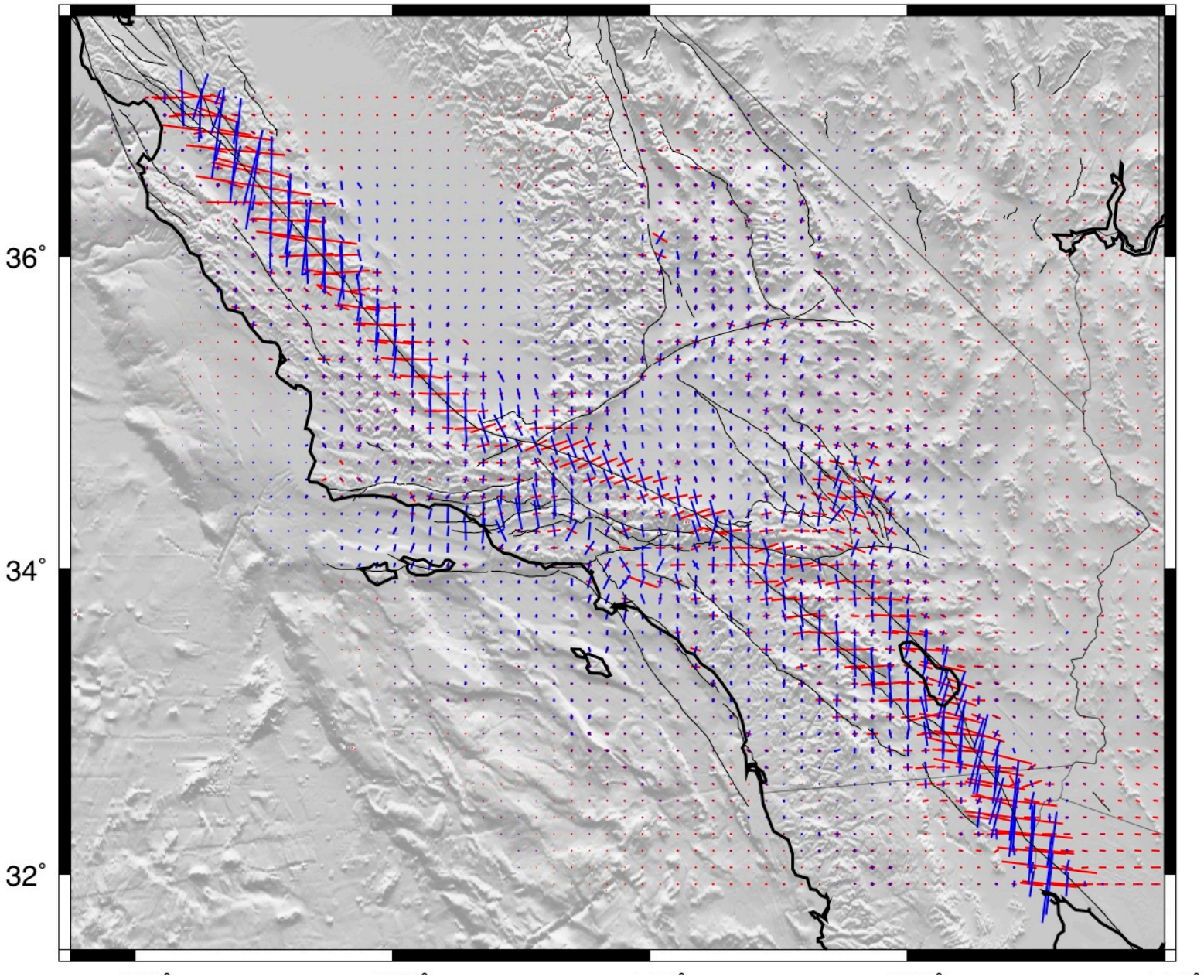

smith_konter

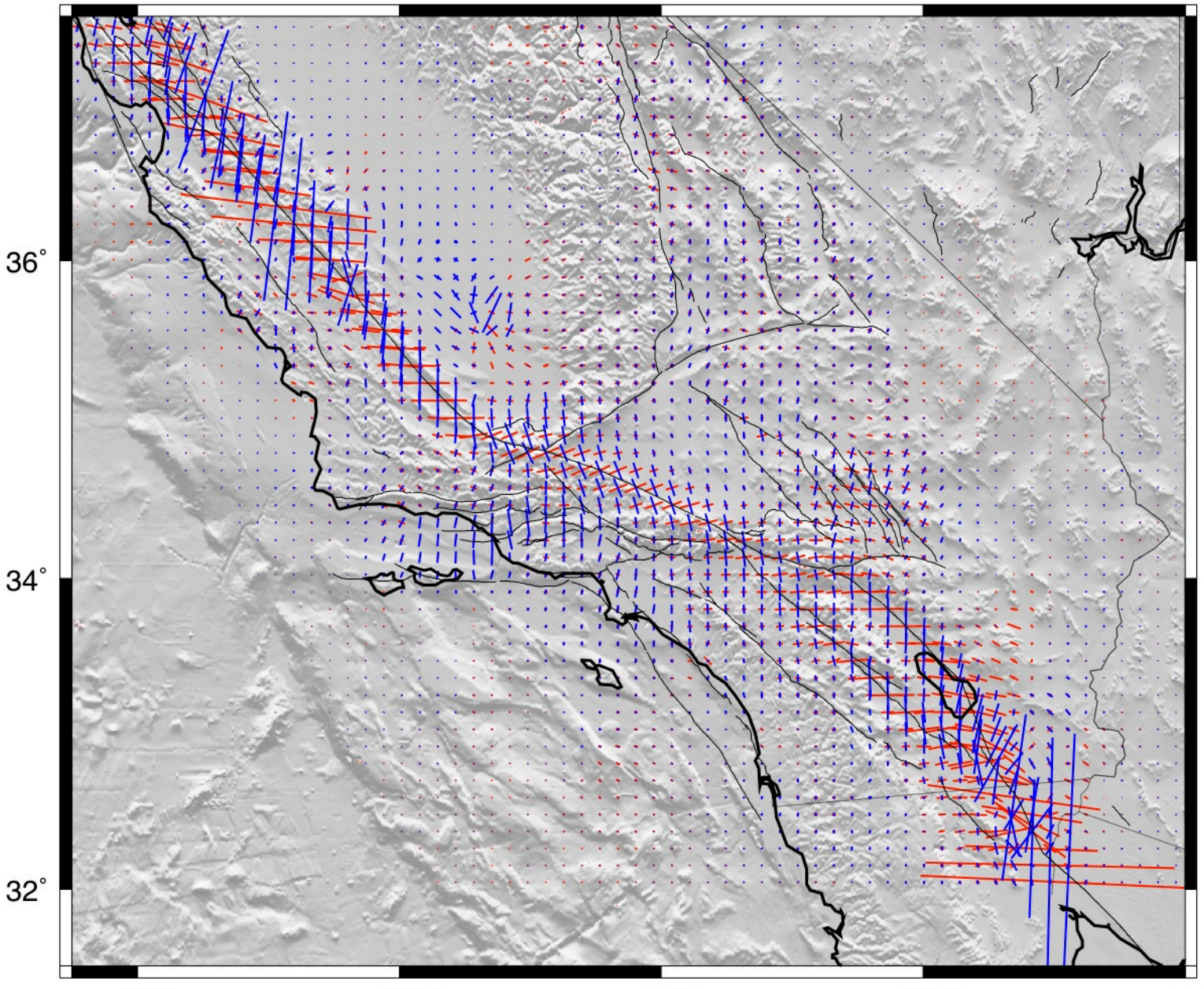

kreemer

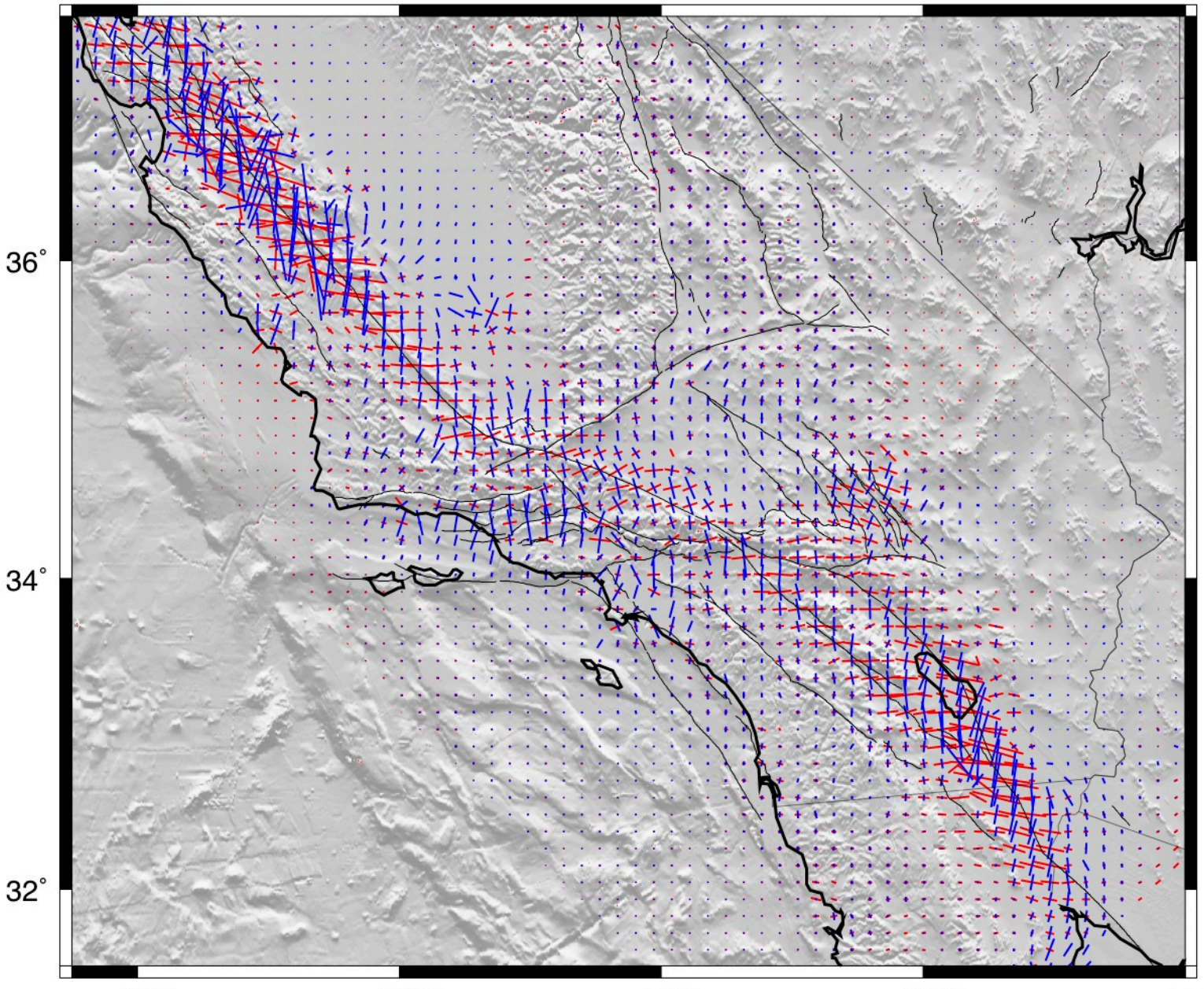

harvard

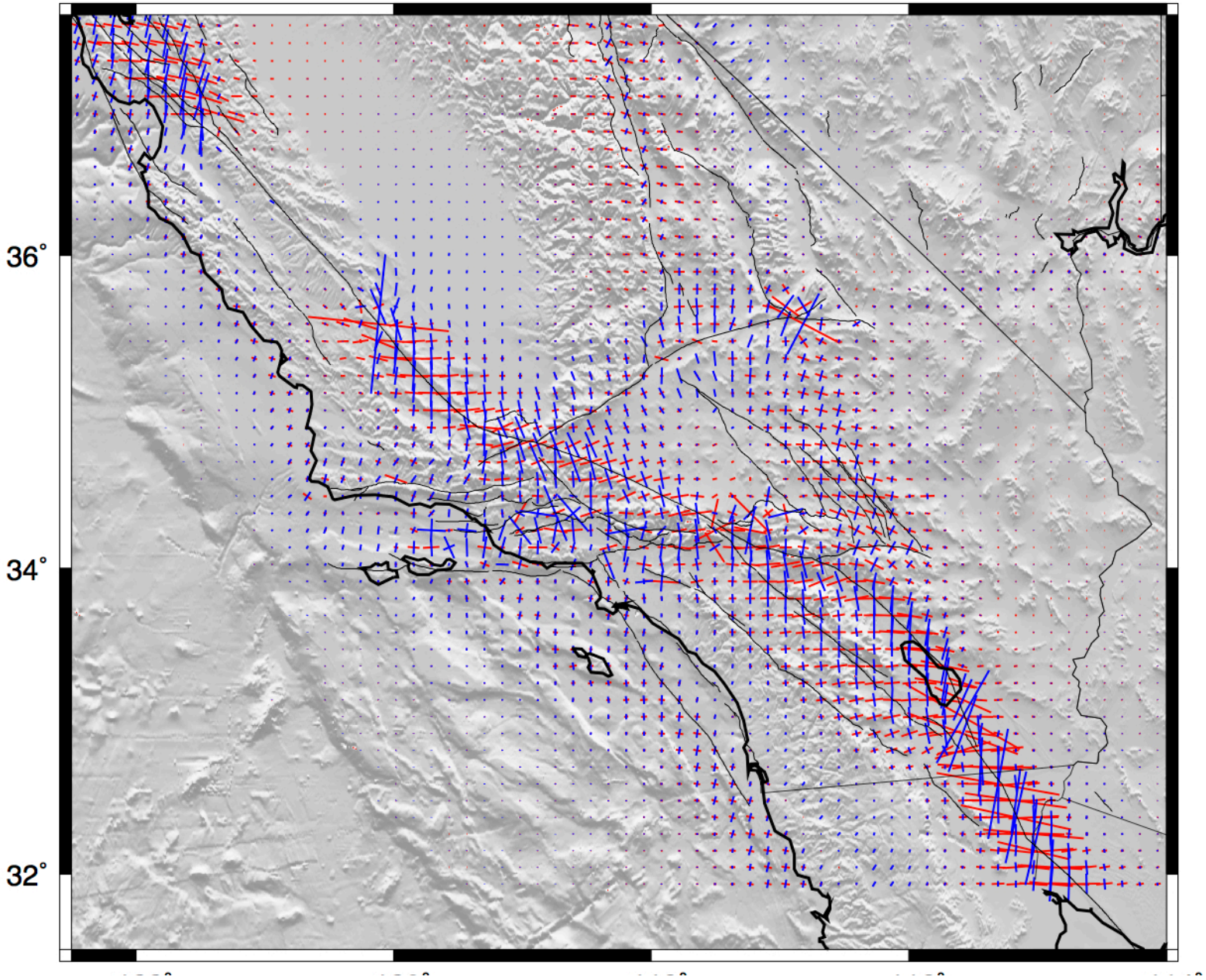

mccaffrey

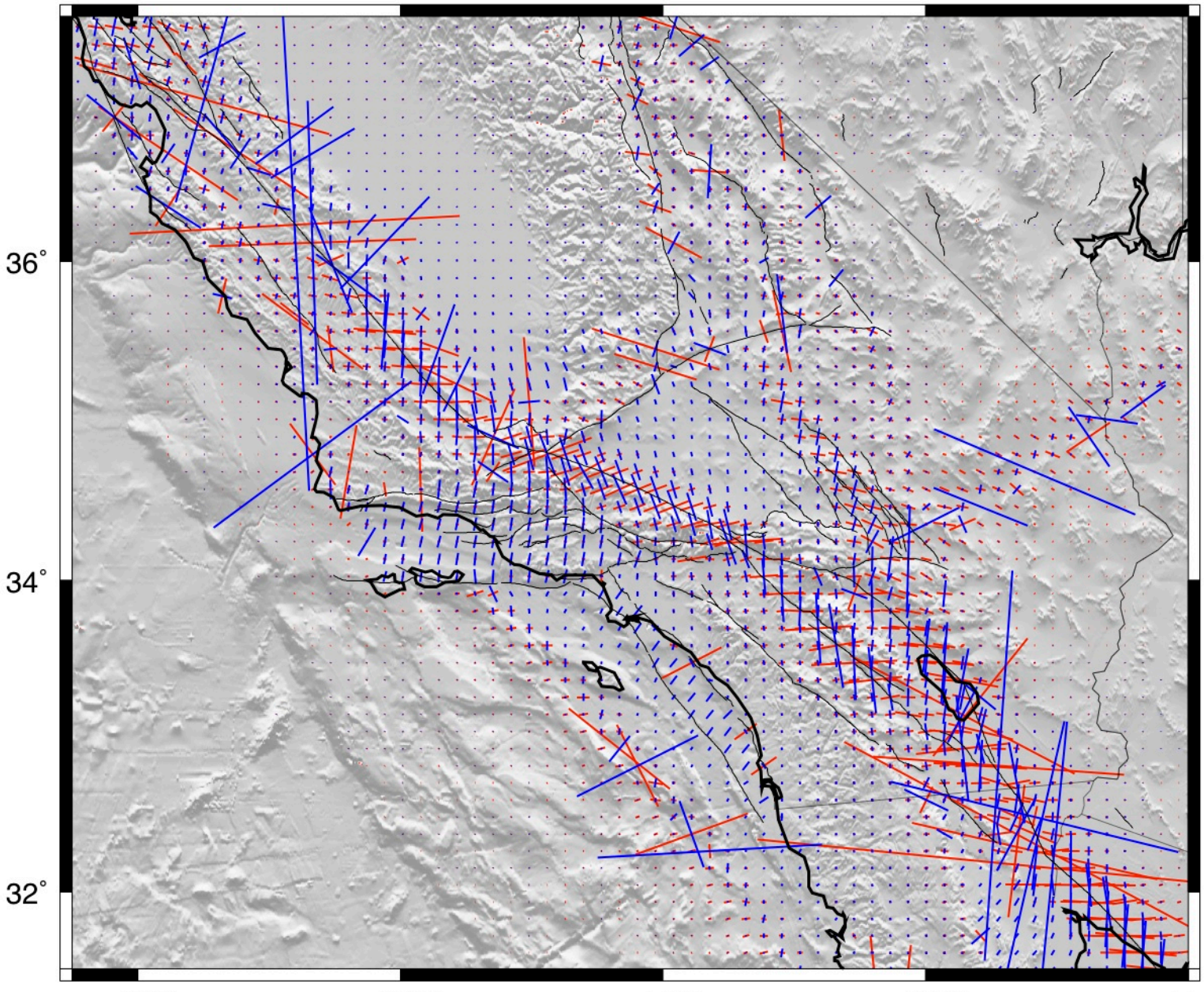

hackl

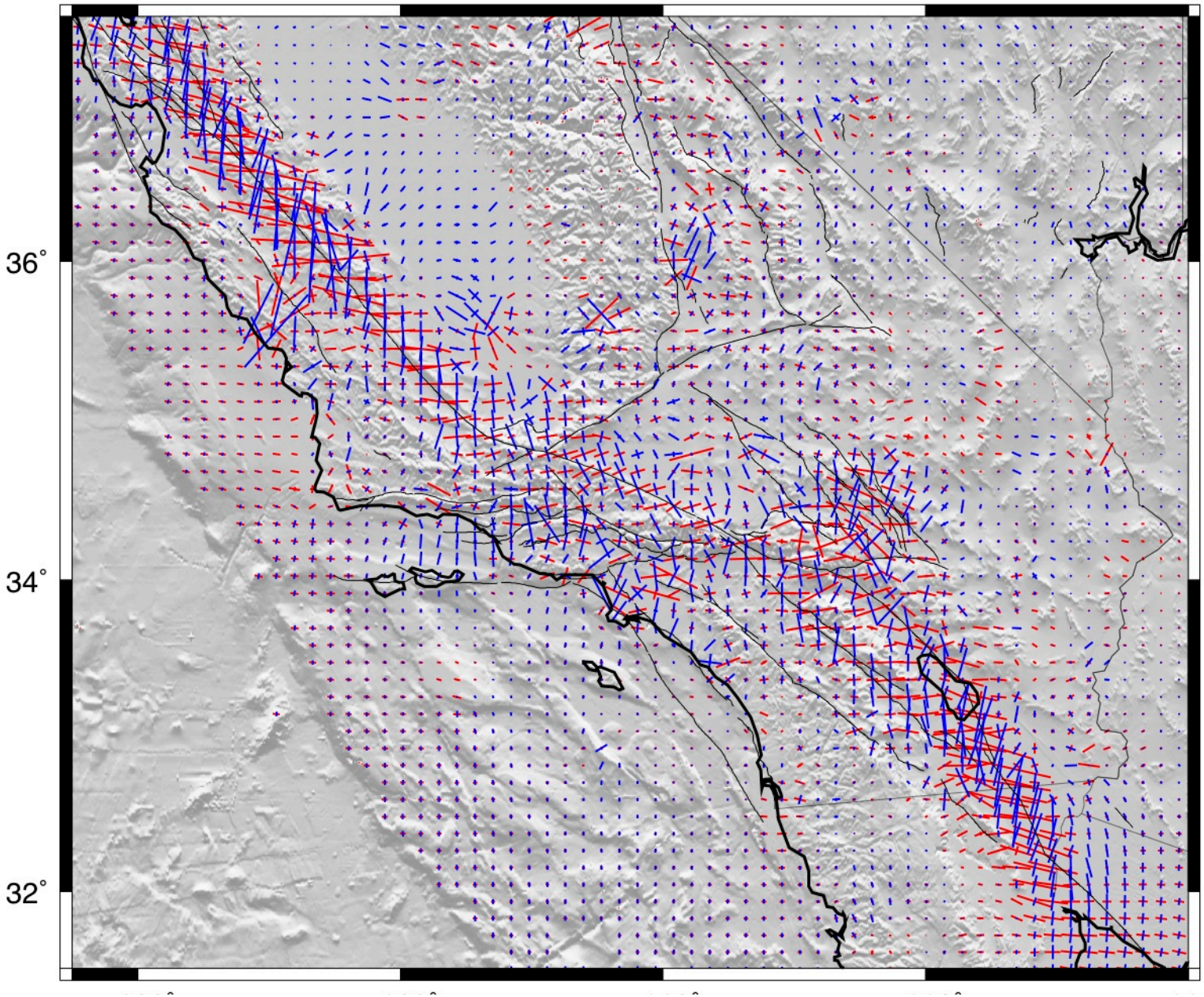

Reconciling Deformation/Stressing Rate Models

Community Stress Workshop
May 29, 2013

Assumptions:
- strain rate can be converted to stress rate using some rheology
- surface stress rate can be downward continued to seismogenic depth

Comparison of 17 strain rate models

Selection of 5 similar models

Coherence analysis of 4 models to establish spatial resolution

Comparison of 4 models with Yang EQ orientations

Where do we go from here?

Comparisons with EQ Orientations prepared by Yang

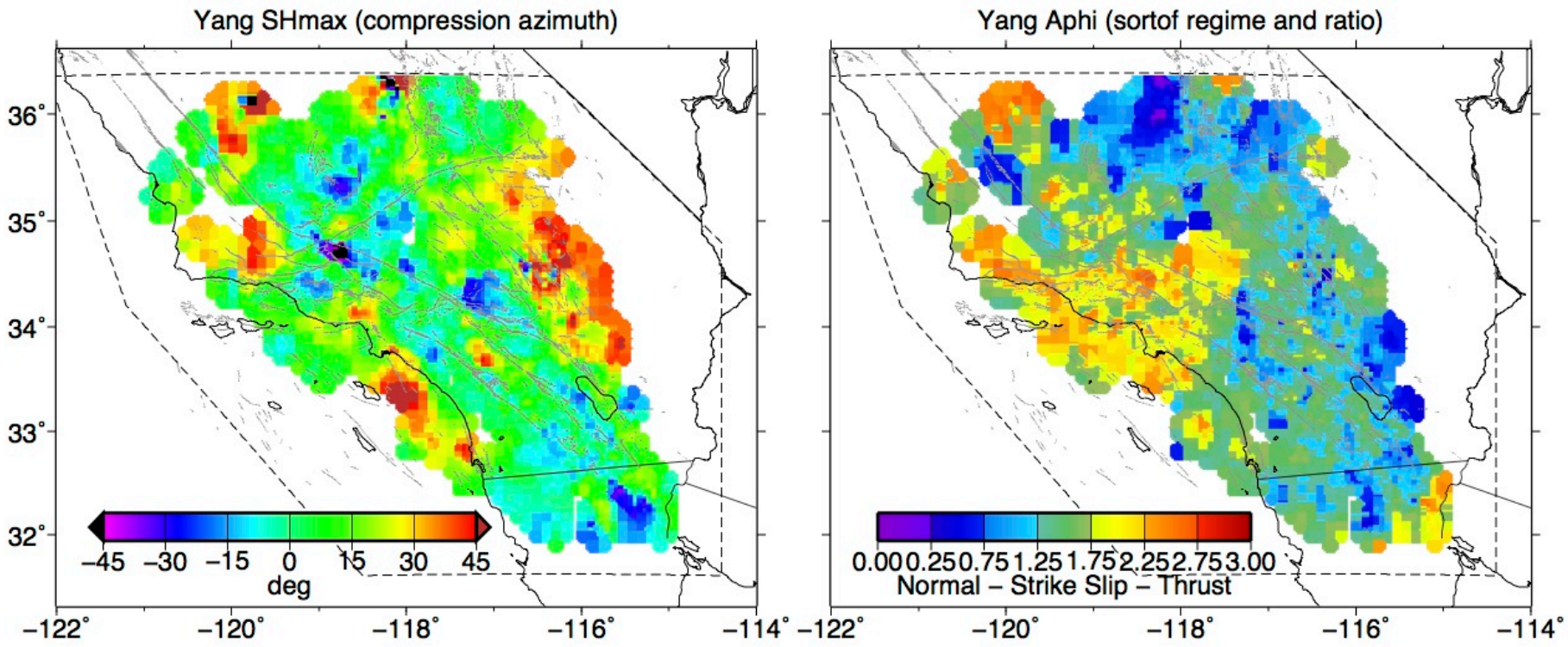

[Analysis by Luttrell and Tong]

Comparisons with EQ Orientations prepared by Yang

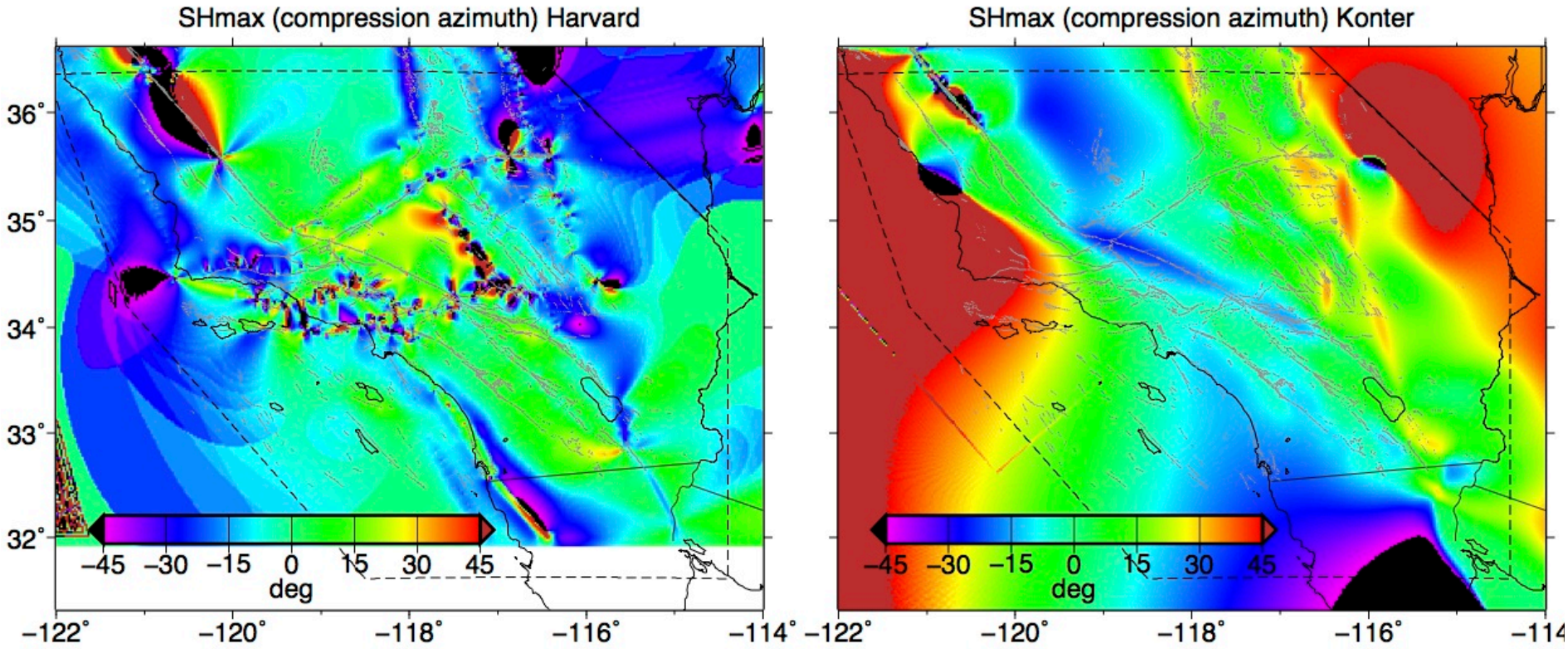

[Analysis by Luttrell and Tong]

Comparisons with EQ Orientations prepared by Yang

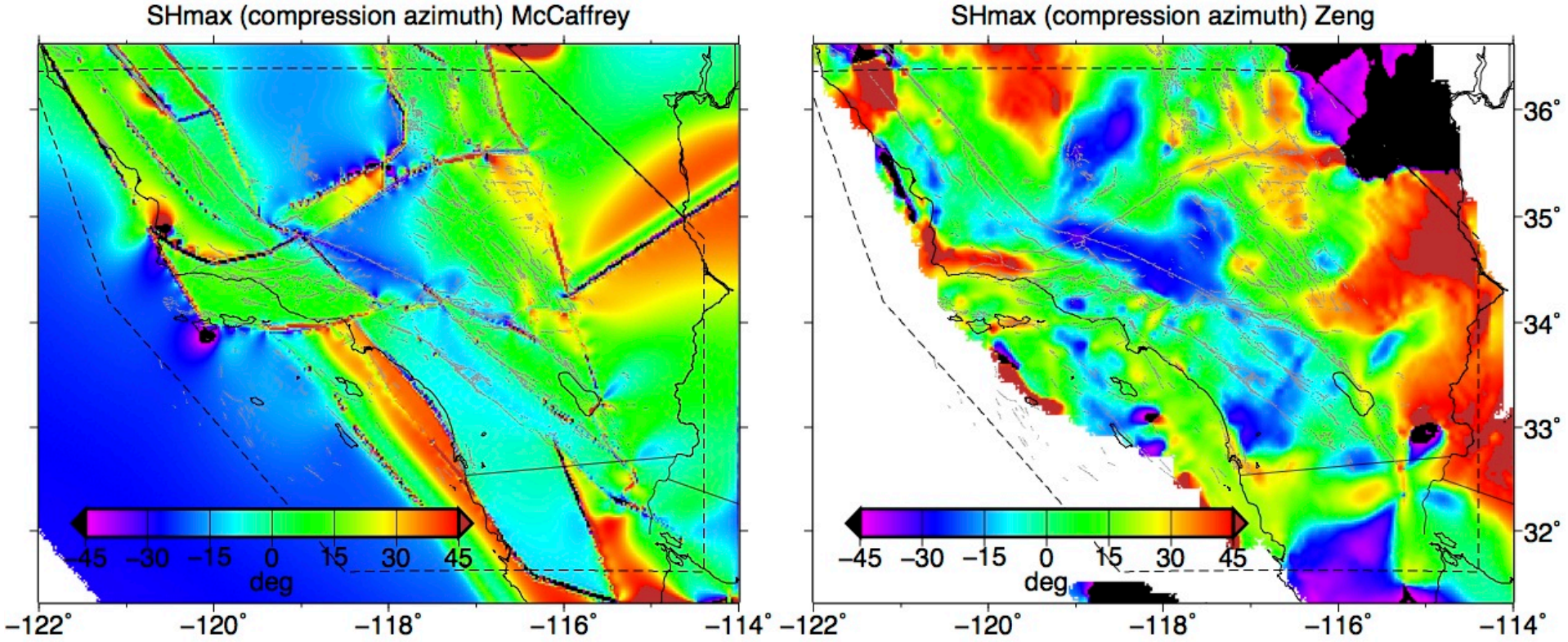

[Analysis by Luttrell and Tong]

Comparisons with EQ Orientations prepared by Yang

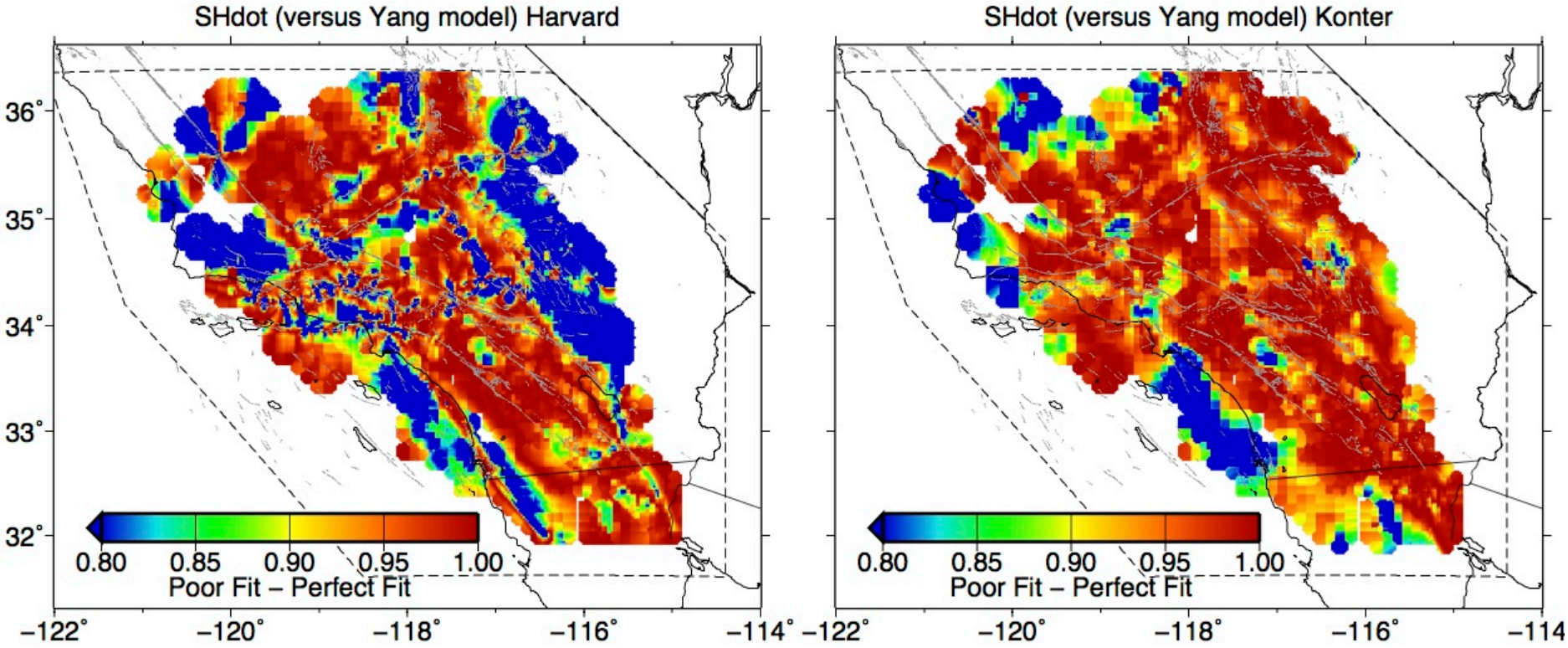

[Analysis by Luttrell and Tong]

Comparisons with EQ Orientations prepared by Yang

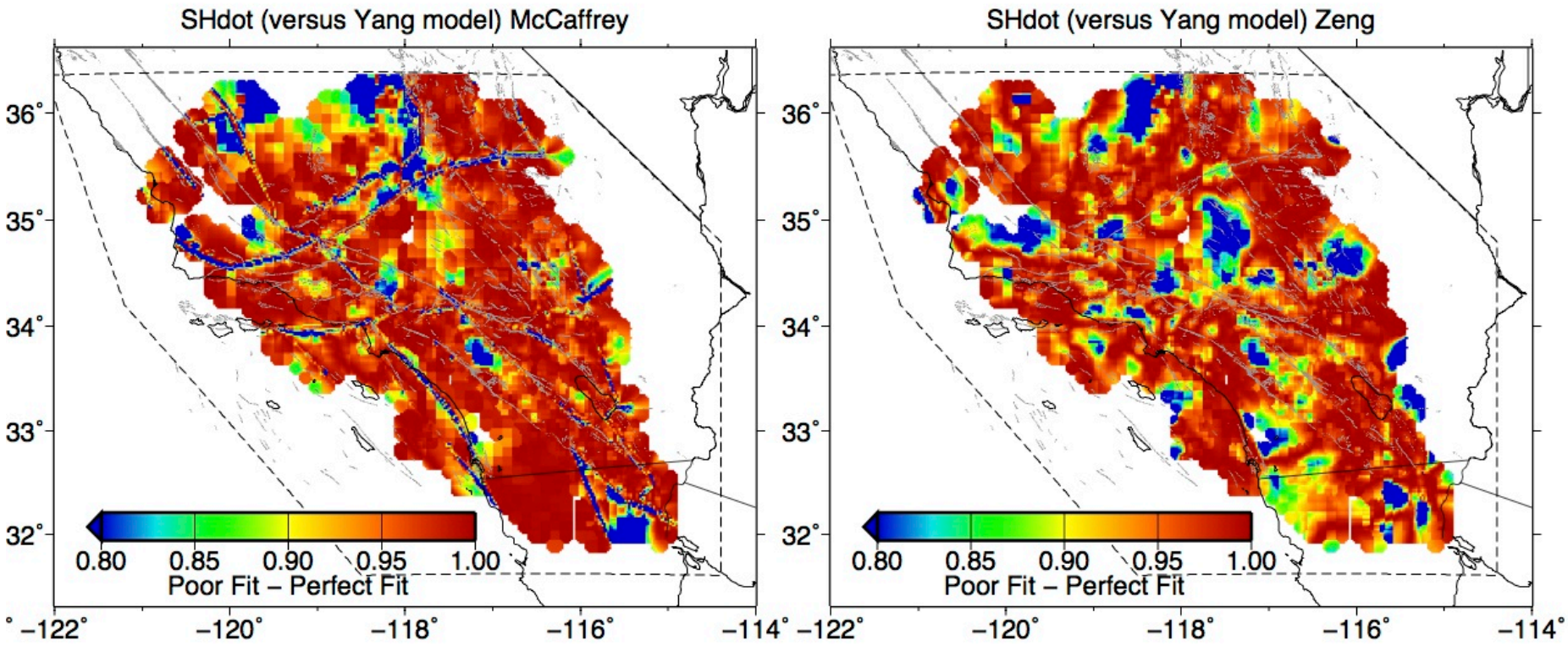

[Analysis by Luttrell and Tong]

Reconciling Deformation/Stressing Rate Models

Community Stress Workshop
May 29, 2013

Where do we go from here?

GPS Spacing does not completely resolve strain rates – need InSAR

A physical model or zome knowledge of fault orientations is needed to properly orient strain rate tensor.

Will the CGM of velocity also serve as a strain rate model for the CSM?

Are the assumptions OK for converting strain-rate to stress-rate?

average of 5 “best” models

mean

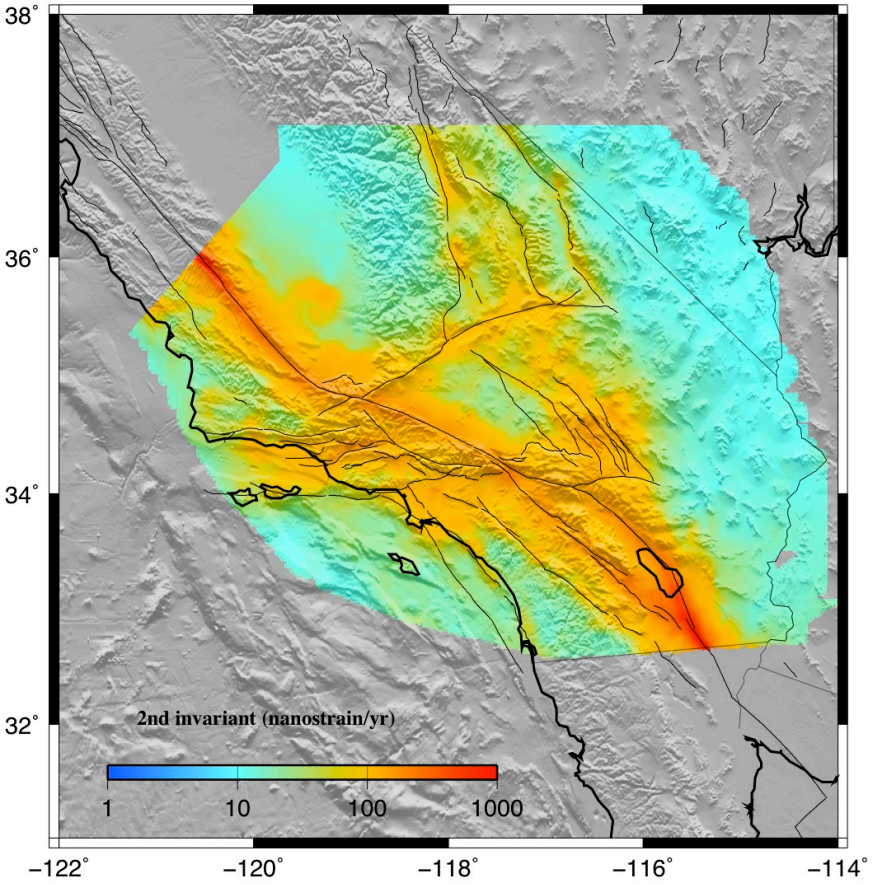

SEISM_strain = $10^{rate+5.3}$

SEISM

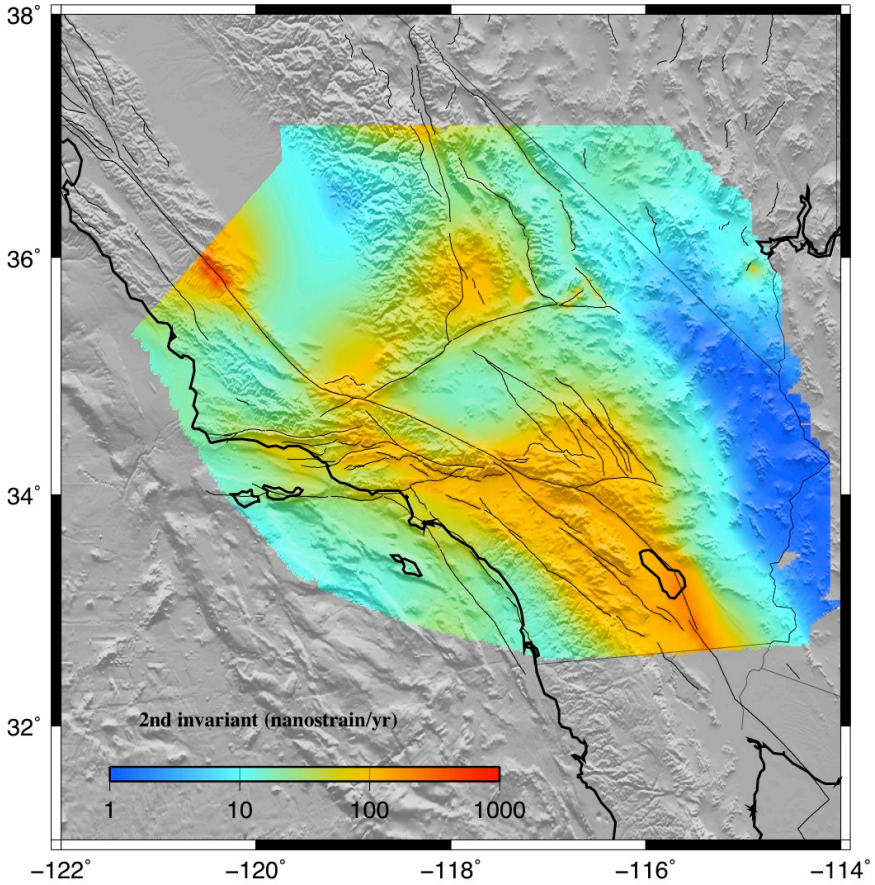

SEISM

The background seismicity model is included to account for M 5.0 - 6.5 earthquakes on faults and for random M 5.0 – 7.0 earthquakes that do not occur on faults included in the model (as in earlier models of Frankel et al., 1996, 2002 and Petersen et al., 1996). We include four different classes of earthquake sources in the California background seismicity model: (1) gridded (smoothed) seismicity, (2) regional background zones, (3) special fault zone models, and (4) shear zones (also referred to as C zones). The gridded (smoothed) seismicity model, the regional background zone model, and the special fault zones use a declustered earthquake catalog for calculation of earthquake rates. Earthquake rates in shear zones are estimated from the geodetically determined rate of deformation across an area of high strain rate. We use a truncated exponential (Gutenberg-Richter, 1944) magnitude-frequency distribution to account for earthquakes in the background models.